JCI The Journal of Clinical Investigation

Type 2 diabetes risk gene Dusp8 regulates hypothalamic Jnk signaling and insulin sensitivity

Sonja C. Schriever, … , Matthias H. Tschoep, Paul T. Pfluger

J Clin Invest. 2020. https://doi.org/10.1172/JCI136363.

Research In-Press Preview **Metabolism**

Graphical abstract

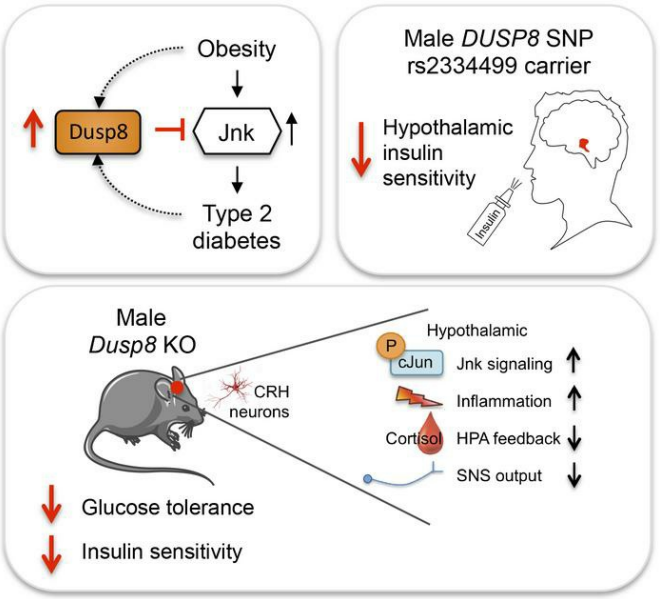

Type 2 diabetes risk gene Dusp8 regulates hypothalamic Jnk signaling and insulin sensitivity

Sonja C. Schriever[1,2,3], Dhiraj G. Kabra[1,2,3,4], Katrin Pfuhlmann[1,2,3,5], Peter Baumann[1,2,3,6], Emily V. Baumgart[1,2,3], Joachim Nagler[7], Fabian Seebacher[2,3,5], Luke Harrison[1,2,3,5], Martin Irmler[8], Stephanie Kullmann[3,9], Felipe Corrêa-da-Silva[10,11], Florian Giesert[12,13], Ruchi Jain[2,3,14], Hannah Schug[15], Julien Castel[16], Sarah Martinez[16], Moya Wu[8], Hans-Ulrich Häring[3,9,17], Martin Hrabe de Angelis[3,8,18], Johannes Beckers[3,8,18], Timo D. Müller[2,3,19], Kerstin Stemmer[2,3], Wolfgang Wurst[12,13,20,21] Jan Rozman[3,8,22], Ruben Nogueiras[23], Meri De Angelis[7], Jeffery D. Molkentin[24,25], Natalie Krahmer[2,3], Chun-Xia Yi[10,11], Mathias V. Schmidt[26], Serge Luquet[16], Martin Heni[3,9,17,27], Matthias H. Tschöp[2,3,5] and Paul T. Pfluger[1,2,3,6,*]

1 Research Unit NeuroBiology of Diabetes, Helmholtz Zentrum München, 85764 Neuherberg, Germany.

2 Institute for Diabetes and Obesity, Helmholtz Zentrum München, 85764 Neuherberg, Germany.

3 German Center for Diabetes Research (DZD), 85764 Neuherberg, Germany.

4 Biological Research Pharmacology Department, Sun Pharma Advanced Research Company Ltd., Vadodara, India.

5 Division of Metabolic Diseases, Technical University of Munich, 80333 Munich, Germany.

6 Neurobiology of Diabetes, TUM School of Medicine, Technical University of Munich, 80333 Munich, Germany.

7 Molecular EXposomics, Helmholtz Zentrum München, 85764 Neuherberg, Germany.

8 Institute of Experimental Genetics and German Mouse Clinic, Helmholtz Zentrum München, 85764 Neuherberg, Germany.

9 Institute for Diabetes Research and Metabolic Diseases of the Helmholtz Center Munich at the University of Tübingen, 72076 Tübingen, Germany.

10 Department of Endocrinology and Metabolism, Amsterdam University Medical Center, University of Amsterdam, 1105AZ Amsterdam, Netherlands.

11 Netherlands Institute for Neuroscience, an Institute of the Royal Netherlands Academy of Arts and Sciences, 1105 BA Amsterdam, Netherlands.

12 Institute of Developmental Genetics, Helmholtz Zentrum München, 85764 Neuherberg, Germany.

13 Department of Developmental Genetics, TUM School of Life Sciences Weihenstephan, Technical University of Munich; c/o Helmholtz Zentrum München, 85764 Neuherberg.

14 Lund University Diabetes Centre, CRC, SUS Malmö, SE-205 02 Malmö, Sweden.

15 SYNLAB Analytics & Services Switzerland AG, 8157 Dielsdorf, Switzerland.

16 Université de Paris, BFA, UMR 8251, CNRS, F-75014 Paris, France.

17 Department of Internal Medicine IV, Division of Endocrinology, Diabetology and Nephrology, University of Tübingen, 72076 Tübingen, Germany.

18 Chair of Experimental Genetics, TUM School of Life Sciences Weihenstephan, Technical University of Munich, 85354 Freising, Germany.

19 Department of Pharmacology and Experimental Therapy, Institute of Experimental and Clinical Pharmacology and Toxicology, Eberhard Karls University Hospitals and Clinics, 72076 Tübingen, Germany.

20 German Center for Neurodegenerative Diseases (DZNE), 81377 München, Germany.

21 Munich Cluster for Systems Neurology (SyNergy), 81377 Munich, Germany.

22 Czech Centre for Phenogenomics, Institute of Molecular Genetics of the Czech Academy of Sciences, 25250 Vestec, Czech Republic.

23 Department of Physiology, University of Santiago de Compostela – Instituto de Investigación Sanitaria, Santiago de Compostela 15782, Spain.

24 Department of Pediatrics, University of Cincinnati, Cincinnati, OH, USA.

25 Howard Hughes Medical Institute, Cincinnati Children's Hospital Medical Center, Cincinnati, OH, USA.

26 Neurobiology of Stress Resilience, Max Planck Institute of Psychiatry, 80804 Munich, Germany.

27 Institute for Clinical Chemistry and Pathobiochemistry, Department for Diagnostic Laboratory Medicine, University Hospital Tübingen, 72076 Tübingen, Germany.

* corresponding author

Contact information:

Dr. Paul T. Pfluger, Research Unit NeuroBiology of Diabetes

Helmholtz Zentrum München GmbH

Ingolstädter Landstraße 1

85764 Neuherberg, Germany

Telefon +49 (0) 89 3187 2104

paul.pfluger@helmholtz-muenchen.de

Abbreviations:

ARC, arcuate nucleus; *GR*, glucocorticoid receptor; GWAS, genome-wide association study; MBH, medio-basal hypothalamus; SNS, sympathetic nervous system

Keywords:

Dual specificity phosphatase 8, T2D, Dusp8-Jnk1 axis, *DUSP8* SNP rs2334499, hypothalamic insulin sensitivity

Abstract

Recent genome-wide association studies (GWAS) identified *DUSP8*, a dual-specificity phosphatase targeting MAP kinases, as type 2 diabetes (T2D) risk gene. Here, we unravel Dusp8 as gatekeeper in the hypothalamic control of glucose homeostasis in mice and humans. Male but not female Dusp8 loss-of-function mice, either with global or CRH neuron-specific deletion, had impaired systemic glucose tolerance and insulin sensitivity when exposed to high-fat diet (HFD). Mechanistically, we found impaired hypothalamic–pituitary–adrenal (HPA) axis feedback, blunted sympathetic responsiveness, and chronically elevated corticosterone levels driven by hypothalamic hyperactivation of Jnk signaling. Accordingly, global Jnk1 ablation, AAV-mediated Dusp8 overexpression in the mediobasal hypothalamus, or metyrapone-induced chemical adrenalectomy rescued the impaired glucose homeostasis of obese male Dusp8 KO mice, respectively. The sex-specific role of murine Dusp8 in governing hypothalamic Jnk signaling, insulin sensitivity and systemic glucose tolerance was consistent with fMRI data in human volunteers that revealed an association of the *DUSP8* rs2334499 risk variant with hypothalamic insulin resistance in men. Further, expression of *DUSP8* was increased in the infundibular nucleus of T2D humans. In summary, our findings suggest the GWAS-identified gene Dusp8 as novel hypothalamic factor that plays a functional role in the etiology of T2D.

Introduction

Obesity-induced insulin resistance is associated with an increase in circulating levels of cytokines and free fatty acids (1) that activate proinflammatory signaling pathways. Mitogen-activated protein kinase (MAPK) signaling (2) plays a major role in this inflammatory process via the sequential, dual phosphorylation and thereby activation of the serine/threonine kinases: c-Jun N-terminal kinase (Jnk), p38 and extracellular signal–regulated kinases (ERK) (2). The magnitude and duration of MAPK signaling dictates the specificity of signal transduction and the extent of biological signaling response (3). MAPKs are thus tightly controlled by MAPK phosphatases (MKP) that form the structurally distinct family of dual-specificity phosphatases (DUSP) (4). The DUSP phosphatases show high homology in an amino-terminal non-catalytic domain and in a carboxyl-terminal catalytic domain, but differ in their substrate specificities, tissue distribution, subcellular localization and inducibility by extracellular stimuli (reviewed in (3, 5)). Recent work using genetic models has revealed potentially important roles of DUSPs in the regulation of pathophysiological signaling with relevance to human diseases including cancer, diabetes, inflammatory and neurodegenerative disorders (4). Here, the cytoplasmic, ERK-specific Dusp6 and Dusp9 and the inducible nuclear and promiscuous, i.e. ERK, JNK and p38-dephosphorylating Dusp1 were reported to modulate glucose homeostasis. Less is known about MKPs specific for JNK and/or p38, namely Dusp8, Dusp10 and Dusp16 given their expression in both the cytoplasm and cell nucleus and their relatively selective substrate specificity (4, 6, 7). Dusp8 appears to be of particular importance for the control of glucose homeostasis based upon recent genome-wide association studies (GWAS) that linked minor allele carriers of the SNP rs2334499 on chromosome 11p15, a region containing *DUSP8* among a number of other genes, with a moderately increased risk for T2D risk (8, 9).

Dusp8 was originally identified as an immediate early gene, and its expression can be stimulated in vitro by nerve growth factor and insulin (10). Expression of *DUSP8* was found to be strong in adult human brain and weak in heart and skeletal muscle (10). Dusp8 over-expression studies revealed greater phosphatase activity against Jnk than p38 or ERK (11). Here we aimed to delineate the functional importance of Dusp8 for the etiology of T2D. We show that *DUSP8* polymorphism rs2334499 is associated with hypothalamic insulin resistance in men and that *DUSP8* expression is increased in the infundibular nucleus of T2D humans. Phenotypic studies in global Dusp8 KO mice

and in Dusp8 KO mice with the hypothalamic rescue of *Dusp8* expression expose a specific role of Dusp8 as gatekeeper for systemic glucose tolerance and insulin sensitivity in an obesogenic environment. Mechanistic studies in Jnk1-Dusp8 double-KO mice and mice with conditional deletion of Dusp8 in CRH neurons further revealed that Dusp8 as Jnk-specific phosphatase acts as regulator for hypothalamic Jnk activation and HPA axis feedback inhibition that is essential for systemic glucose homeostasis.

Results

Expression levels of Dusp8 are upregulated in the hypothalamus of mice by body adiposity.

We first aimed to investigate the murine expression pattern of *Dusp8*, the product of a gene recently linked with an increased risk for T2D in humans (8, 9). Focusing on tissues relevant for glucose tolerance in mice, we largely confirmed earlier reports showing high expression levels of *DUSP8* in adult human brain, heart and skeletal muscle (10). Specifically, we showed high expression levels of *Dusp8* in several brain areas including the hypothalamus, and considerable expression in selected types of skeletal muscle of mice (**Figure 1A**). We next assessed the impact of nutrient overload on *Dusp8* gene expression in vivo in HFD-fed diet-induced obese (DIO) mice. *Dusp8* expression was not altered in muscle (**Figure 1B**) but significantly increased in hypothalami of DIO mice (**Figure 1C**). In contrast, prolonged fasting, which is known to mobilize massive amounts of free fatty acids into circulation, and re-feeding by fat free diet (FFD) or HFD had no impact on hypothalamic *Dusp8* gene expression (**Figure 1D**). Moreover, hypothalamic *Dusp8* expression was also increased in genetically obese, chow-fed Lep^{ob} mice (**Figure 1E**) but unaffected by leptin replacement therapy (data not shown). These data indicate that the transcriptional regulation of *Dusp8* in mice is independent from leptin signaling or dietary fatty acids. In situ hybridizations revealed that *Dusp8* expression is increased in the medio-basal hypothalamus (MBH), a region known for the regulation of glucose and energy homeostasis, of Lep^{ob} mice compared to WT controls (**Figure 1F-H)**. Overall, we show that hypothalamic *Dusp8* expression appears to be regulated by body adiposity, a metabolic state that often correlates with impaired glucose homeostasis.

Global ablation of Dusp8 exacerbates HFD-induced glucose intolerance specifically in male mice.

To explore whether Dusp8 has indeed a gluco- and energy-regulatory function in vivo we studied mice with global ablation of Dusp8. Male and female Dusp8 KO mice that were fed a standard chow diet neither showed a difference in body weight or body composition nor displayed glucose or insulin intolerance compared to their respective WT controls (**Supplemental Figure 1**). After inducing nutrient overload and obesity by 12 weeks of HFD feeding, we found comparable changes in body weight and body composition (**Figure 2A,B**) as well as unperturbed food intake, energy expenditure,

respiratory exchange ratios, locomotor activity and leptin sensitivity (**Supplemental Figure 2)** in male Dusp8 WT and KO mice**.** However, despite similar propensities for diet-induced obesity, male Dusp8 KO mice exposed to HFD showed an impairment of glucose homeostasis in a glucose tolerance test (GTT) (**Figure 2C,D)**. In a pyruvate tolerance test (PTT), we found increased baseline glucose levels after overnight fasting and impaired glucose clearance in HFD-fed Dusp8 KO males (**Figure 2E,F)**. An insulin tolerance test (ITT) revealed a decrease in insulin sensitivity in obese Dusp8 KO males (**Figure 2G,H)**. Male mice heterozygous for the Dusp8 deletion showed similar glucose tolerance and insulin sensitivity as WT littermates after HFD exposure (data not shown). In male HFD-fed Dusp8 KO mice fasting plasma insulin levels (WT: 36.5 ± 12.0 µU/ml; Dusp8 KO: 67.0 ± 10.4 µU/ml) and HOMA-IR (**Figure 2I)** indices were significantly higher compared to their WT counterparts. Plasma markers for lipid metabolism (**Supplemental Figure 3A-C)** and hepatic triglyceride stores (**Supplemental Figure 3D)** were comparable between HFD-fed Dusp8 WT and KO males. An intravenous (iv) GTT revealed higher insulin secretion in obese Dusp8 KO males compared to WT controls (**Figure 2J,K**), which points towards insulin resistance in Dusp8 KO males. In ex vivo analyses in isolated beta cells of male Dusp8 WT and KO mice, we found comparable insulin content (**Supplemental Figure 3E)** and glucose-stimulated insulin secretion (**Supplemental Figure 3F)**. Combined, these data suggest impaired insulin sensitivity instead of insulin secretory problems in HFD-fed Dusp8 KO males. Female Dusp8 WT and KO mice showed comparable susceptibilities to gain body weight (**Supplemental Figure 3G)** and body fat (**Supplemental Figure 3H)** when fed HFD. Similarly, neither glucose tolerance nor insulin sensitivity were affected by Dusp8 ablation in HFD-fed female mice (**Supplemental Figure 3I-L)**. Taken together, these data indicate impaired glucose tolerance and insulin resistance in male but not female Dusp8 KO mice exposed to HFD.

Glucose intolerance in obese global Dusp8 KO mice can be reversed by hypothalamic Dusp8 overexpression.

Next, we aimed to assess the specific role of hypothalamic Dusp8 by injecting Dusp8 overexpressing adeno-associated virus (Dusp8 AAV) into the mediobasal hypothalamus (MBH) of WT mice resulting in a 4-fold higher hypothalamic *Dusp8* expression, compared to green fluorescent protein (GFP)-AAV-injected controls (**Figure 2L,M**). AAV-mediated over-expression of Dusp8 in the MBH had no

effect on glucose tolerance in HFD-fed WT male mice compared to GFP controls (**Figure 2N,O**). However, overexpression of Dusp8 in the MBH of global Dusp8 KO males significantly improved their impaired glucose tolerance and normalized their glucose levels to HFD-fed WT males (**Figure 2N,O**). None of the groups displayed changes in body weight or body composition in response to AAV treatment (data not shown). The rescue of glucose intolerance by AAV-mediated Dusp8 overexpression in the MBH points towards a central hypothalamic role of Dusp8 in regulating glucose homeostasis in an obesogenic environment.

Impaired hypothalamic insulin sensitivity, elevated glucocorticoid signaling and reduced sympathetic responsiveness in HFD-fed Dusp8 KO males.

The impaired glucose tolerance in Dusp8 KO males was reflected by aberrant expression levels of key enzymes involved in glucose uptake, glycolysis, glycogen synthesis and glycogen breakdown in liver and skeletal muscle of HFD-fed Dusp8 KO mice, compared to WT controls (**Figure 3A,B**). In an acute insulin challenge test, we moreover observed reduced hypothalamic Akt phosphorylation in HFD-fed Dusp8 KO males relative to WT controls which indicates impaired hypothalamic insulin responsiveness (**Figure 3C,D)**. In the hypothalamus, we further observed increased expression levels of arginine vasopressin (*Avp*), oxytocin (*Oxt*) and corticotropin releasing hormone (*CRH*). Elevated *CRH* mRNA levels in the hypothalamus were reflected by increased adrenocorticotropin hormone (*Acth*) and Crh receptor 1 (*Crhr1*) expression in the pituitary as well as steroid synthesis enzymes in the adrenals (**Figure 3E**). Expression levels of glucocorticoid signaling components in liver, muscle and hypothalamus were also increased (**Figure 3F-H**), thus indicating elevated glucocorticoid action in HFD-fed Dusp8 KO males.

Increased glucocorticoid action in humans has recently been associated with an impaired sympathetic outflow (12) and lower norepinephrine (NE) levels (13), thereby impeding systemic glucose control to systemically drive glucose intolerance (14). Consistent with these human data, we observed lower baseline NE levels in livers of Dusp8 KO males compared to WT mice (**Figure 3I**; 0 hours). In contrast, NE baseline levels were unaltered in soleus muscle and pancreas of Dusp8 KO mice (**Figure 3J,K**; 0 hours). However, the application of a single dose of tyrosine hydroxylase inhibitor α-MPT (15) revealed decreased NE turnover rates in livers, muscle and pancreas of Dusp8 KO mice (**Figure**

3L-N). In contrast to the HFD-fed Dusp8 KO males, female Dusp8 KO mice did not display deregulated glucose metabolism or elevated glucocorticoid action when exposed to HFD (**Supplemental Figure 4),** which is in agreement with their unaffected glucose tolerance and insulin sensitivity. Overall, the data point towards blunted sympathetic responsiveness as consequence of increased glucocorticoid action in HFD-fed male Dusp8 KO mice.

Blunted HPA axis feedback control in Dusp8 deficient male mice.

Consistent with the elevated expression of glucocorticoid receptor (GR) target genes, we found increased basal corticosterone levels measured 2 hours after the onset of the light phase (9 am) in HFD-fed Dusp8 KO males compared to WT controls (**Figure 4A)**. Increased glycogen storage in livers of HFD-fed Dusp8 KO mice (**Figure 4B)** and our recent finding of decreased hippocampal mass in Dusp8 KO males (16) were further indicators for chronic hypercorticosteronemia driven by Dusp8 deficiency. The absence of a marked adrenal hypertrophy in HFD-fed Dusp8 KO mice compared to WT controls (**Figure 4C)** suggested a dysfunctional HPA axis feedback at the level of the hypothalamus or the pituitary as cause for the observed increased basal corticosterone levels. A combined dexamethasone suppression / CRH stimulation test (Dex/CRH) (17) revealed diminished suppression of corticosterone production after low dose dexamethasone administration in HFD-fed Dusp8 KO mice (**Figure 4D)**. Peripheral injection of CRH induced a robust increase of corticosterone concentrations, which was significantly more pronounced in Dusp8 KO mice compared to WT controls. Taken together, these data indicate compromised GR-mediated negative feedback at the level of the hypothalamus and at the pituitary, possibly due to a hypothalamic CRH overdrive.

Chemical adrenalectomy normalizes glucose tolerance in HFD-fed Dusp8 KO mice.

To determine whether hypercorticosteronemia is causally driving the observed glucose intolerance in HFD-fed Dusp8 KO mice, we blocked endogenous corticosterone production by metyrapone treatment (18). Following this widely used method of chemical adrenalectomy, we found a normalization of the glucose intolerance phenotype, with comparable glucose excursions and AUC levels for male WT and Dusp8 KO mice after 14 days of metyrapone treatment (**Figure 4E,F**). Metyrapone treatment was further sufficient to normalize gene expression of key genes involved in

T2D pathophysiology and multiple glucocorticoid target genes (**Supplemental Figure 5A-G**). Prior to metyrapone treatment, we confirmed glucose intolerance in our cohort of HFD-fed Dusp8 KO mice compared to WT controls (**Supplemental Figure 5H,I**). We furthermore found no effect of metyrapone treatment on body weight (**Supplemental Figure 5J**). The normalization of glucose tolerance and peripheral glucoregulatory gene profiles by metyrapone treatment suggests that the elevated basal cortisol concentrations are causal for the dysregulation of glucose homeostasis in Dusp8 KO mice.

Hypercorticosteronemia and glucose intolerance in CRH neuron-specific Dusp8 KO mice.

Given the increased hypothalamic expression of CRH and the blunted HPA axis feedback control indicating CRH overdrive from the hypothalamus in HFD-fed global Dusp8 KO mice, we next investigated whether the conditional ablation of Dusp8 in CRH-producing neurons (**Figure 4G**) can recapitulate the glucose intolerance and hypercorticosteronemia phenotype of the global Dusp8 KO mice. Male Dusp8$^{CRH\text{-}Cre}$ WT and KO mice had similar body weight and body composition after exposure to HFD for 12 weeks (**Figure 4H,I**). As hypothesized, ablation of Dusp8 specifically in CRH neurons indeed impaired glucose tolerance (**Figure 4J,K**) and insulin sensitivity (**Figure 4L,M**) in HFD-fed mice. Plasma insulin levels (WT: 267.7 ± 58.5 µU/ml; Dusp8 KO: 325.6 ± 56.0 µU/ml; p=0.0277) and HOMA-IR (**Figure 4N)** indices were significantly higher in male Dusp8$^{CRH\text{-}Cre}$ KO mice on HFD compared to their WT counterparts. Further, we found increased basal corticosterone levels in Dusp8$^{CRH\text{-}Cre}$ KO mice compared to WT controls (**Figure 4O**).

Given that the impairments in glucose tolerance and insulin sensitivity appeared milder in the Dusp8$^{CRH\text{-}Cre}$ KO mice compared to global Dusp8 KO mice, we hypothesized a glucoregulatory role of Dusp8 also in other neuronal subpopulations in the hypothalamus. We thus generated mice with a conditional ablation of Dusp8 in AgRP- or POMC neurons. Both hypothalamic neuronal populations are essential for metabolic homeostasis (19), interconnections of AgRP neurons with CRH neurons are moreover linked with stress regulation and energy homeostasis (20). However, we did not reveal any alterations in the susceptibilities to diet-induced weight or fat mass gain, glucose or insulin tolerance or corticosterone levels between HFD-fed male Dusp8$^{AgRP\text{-}Cre}$ WT vs. KO males (**Supplemental Figure 6A-G**) or Dusp8$^{POMC\text{-}Cre}$ WT vs. KO males (**Supplemental Figure 6H-N**). Overall, these

results suggest a prominent role of Dusp8 in CRH neurons in the regulation of HPA axis reactivity, plasma corticosterone levels and glucose homeostasis.

Dusp8 is a gatekeeper for Jnk activity and Jnk- dependent regulation of GR activity.

To identify the signaling pathway mediating the impaired glucose tolerance and HPA axis feedback inhibition in our Dusp8 loss-of-function mice, we initially assessed the phosphatase activity of Dusp8 towards the MAP kinases Jnk, p38 and ERK using an in vitro model of Dusp8 overexpression. Exposure of cells to the general MAPK activator and ER stressor anisomycin showed that overexpression of Dusp8 abolished the phosphorylation of Jnk and partially p38 (**Figure 5A-D**). Notably and despite recent evidence suggesting a role for Dusp8 in ventricular remodeling via altering ERK1/2 activity (21), we found unaltered ERK phosphorylation in Hek293 cells stimulated with anisomycin (**Figure 5A,E**). Overall, these data indicate that Dusp8 shows highest phosphatase activity towards Jnk, weaker activity towards p38, and no activity towards ERK in cells stimulated by anisomycin.

In the past, Jnk hyperactivation was shown to impair GR activity via phosphorylation at the inhibitory site Ser226 (22). First, we corroborated that anisomycin treatment increases Jnk activity as well as GR phosphorylation at the inhibitory Ser226 residue (**Figure 5F)**. We then found that overexpression of Dusp8 abolishes both Jnk activation as well as GR^{Ser226} phosphorylation (**Figure 5F,G**). In a GR luciferase reporter assay, we further revealed functional relevance for the protective role of Dusp8 in a Jnk-driven GR^{Ser226} phosphorylation. Overexpression of Dusp8 had no effect on basal, dexamethasone-induced stimulation of GR activity (**Figure 5H**). Addition of the stressor anisomycin massively repressed the transcriptional activity of GR (**Figure 5I**), but the Jnk-mediated downregulation of GR activity was ameliorated by Dusp8 overexpression (**Figure 5I**). These data indicate that a reduction of Jnk activity by Dusp8 signaling can augment GR-dependent transcription.

Next, we assessed the effect of Dusp8 ablation on MAPK phosphorylation in our Dusp8 KO mouse model (**Figure 5J-P**). Due to the unavailability of a specific antibody against Dusp8 (**Supplemental Figure 7**), genotypes were confirmed by PCR analysis. Phosphorylation of the Jnk downstream target cJun was upregulated in the hypothalamus of HFD-fed Dusp8 KO males compared to WT controls (**Figure 5J,L**) along with elevated total protein levels of Jnk and cJun (**Figure 5J,O,P**). In muscle of

HFD-fed mice the phosphorylation of MAPK was barely detectable (**Supplemental Figure 8A,B)**. In livers of Dusp8 KO males we found increased phosphorylation of Jnk and cJun (**Supplemental Figure 8C,D)**, whereas no differences were detected for epididymal white adipose tissue (eWAT) (**Supplemental Figure 8E,F)**. In line with the in vitro results in cells, we found a trend towards increased GR phosphorylation at the inhibitory Ser226 residue in the hypothalamus of Dusp8 KO mice (**Figure 5Q,R)**. GR^{Ser226} phosphorylation was significantly increased in muscle, but decreased in liver and unaltered in eWAT of Dusp8 KO mice (**Supplemental Figure 8G-L)**. Hypothalamic phospho-proteome analyses revealed an overall increase in the number of phosphorylated peptides in Dusp8 KO males compared to WT controls (**Supplemental Figure 8M**), but due to a relatively low abundance we could not detect any significantly deregulated MAPK phospho-sites in the hypothalamus of Dusp8 KO males (**Supplemental Figure 8N, Supplemental Table 1**). Combined, these results confirm substrate preference of Dusp8 for Jnk, but also indicate a putative crosstalk between MAPK. Overall, our data suggest an important protective role of Dusp8 as gatekeeper for hypothalamic Jnk signaling, the Jnk-dependent negative feedback inhibition of hypothalamic GR signaling and glucocorticoid action.

Jnk1 co-deletion normalizes glucose tolerance and hypercorticosteronemia in HFD-fed Dusp8 KO mice.

Hypothalamic phosphatase activity of Dusp8 for Jnk was especially high in the arcuate nucleus (ARC), a major hypothalamic center governing energy and glucose homeostasis, measured by increased phosphorylation of c-Jun in HFD-fed mice with global ablation of Dusp8 compared to WT controls (**Figure 6A-C)**. The number of nuclei with phosphorylated cJun were also increased in the ARC of HFD-fed male $Dusp8^{CRH\text{-}Cre}$ KO mice compared to WT controls (**Supplemental Figure 9**). Microarray analyses of laser-capture-microdissected ARC from HFD-fed global Dusp8 WT and KO confirmed alterations in MAPK and GR signaling in Dusp8 KO males relative to WT controls (**Figure 6D,E; Supplemental Table 2**). We further observed an enrichment of deregulated genes involved in neuro-inflammation, insulin action as well as AMPK, LXR/RXR, PI3K, PKA and STAT3 signaling. Single cell expression data suggested a mostly neuronal role of Dusp8 (23), which was in line with the absence of microgliosis or astrocytosis in Dusp8 global KO males on HFD (**Supplemental Figure**

10).

To corroborate that glucose intolerance of Dusp8 KO males is driven by altered Jnk activity, we generated global Jnk1-Dusp8 double knockout (dKO) mice. When fed chow diet, WT, Dusp8 KO, Jnk1 KO and Jnk1-Dusp8 dKO males displayed comparable body weights and body composition, unchanged glucose tolerance and insulin sensitivity in all genotypes (**Supplemental Figure 11**). Upon exposure to HFD, Jnk1 KO mice were protected from diet-induced obesity (**Figure 6F-H**) as published previously (24). Body weights and body composition of Jnk1-Dusp8 dKO mice on HFD were unaltered compared to Jnk1 KO mice but showed a tendency to be reduced when compared to Dusp8 KO mice and WT controls (**Figure 6F,G**). Consistent with the high hypothalamic Jnk activity in Dusp8 KO males on HFD, the hypothalamic expression of inflammatory markers *Emr1, Ikkb, IL1b* and *Nfkb* was increased in Dusp8 KO males on HFD but reversed when Jnk1 was co-deleted in Dusp8 KO mice (**Figure 6I)**. In line with the known role of hypothalamic Jnk as regulator of systemic glucose homeostasis (25), co-deletion of Jnk1 in Dusp8 KO mice on HFD improved glucose tolerance (**Figure 6J,K**) and insulin sensitivity (**Figure 6L,M**) compared to Dusp8 KO mice. The improvements in glucose homeostasis in Jnk1-Dusp8 dKO mice were reflected by improved fasting insulin (**Figure 6N**) and HOMA-IR values (**Figure 6O)** relative to Dusp8 KO mice. We further revealed that the increased Jnk activity in the global Dusp8 KO mice was causally driving the observed hypercorticosteronemia as Jnk1-Dusp8 dKO mice on HFD showed normalized plasma corticosterone levels (**Figure 6P**).

Finally, as p38 MAPK is another potential target of Dusp8 (11), we co-inserted a dominant-negative p38 allele into global Dusp8 KO mice, which led to hypomorphic p38 activity (26), but had no effect on impaired glucose tolerance in HFD-fed Dusp8 KO mice (**Supplemental Figure 12**). Overall, our results demonstrate that co-deletion of Jnk1 in Dusp8 KO mice reverses the hypothalamic inflammation and impaired glucose tolerance and insulin sensitivity observed in HFD-fed Dusp8 KO mice. This finding is consistent with several reports showing that decreasing Jnk activity sensitizes insulin metabolic actions (24, 25, 27, 28).

Hypothalamic insulin resistance in humans carrying the *DUSP8* diabetes-risk allele.

After revealing a regulatory role of Dusp8 in the control of glucose homeostasis in mice, we next aimed to translate our findings to humans by first assessing the hypothalamic *DUSP8* expression in human brain tissue collected by the Netherlands Brain Bank (29). In the infundibular nucleus of T2D patients the expression of *DUSP8* was significantly increased compared to non-diabetic control subjects (**Figure 7A**).

Next, we assessed the hypothalamic insulin sensitivity of human carriers of the minor T allele in the intergenic T2D risk variant rs2334499. Built on our recent work that established a reduced cerebral blood flow (CBF) after nasal insulin as a marker of high hypothalamic insulin sensitivity (30), we used magnetic resonance imaging to quantify CBF in the hypothalamus (**Figure 7B**) before and 15 min after application of intranasal insulin in 47 volunteers (**Supplemental Table 3**). The insulin-induced change in hypothalamic blood flow was significantly associated with the *DUSP8* SNP rs2334499 with a stronger insulin-dependent suppression of CBF in major C allele carriers (C/C) (p=0.0345, adjusted for sex; p=0.0334, adjusted for sex, age, BMI) shown by the lower values of change in hypothalamic CBF levels compared to heterozygous (C/T) or minor T allele carriers (T/T) (**Figure 7C).** Stratification by sex then revealed that this association between impaired hypothalamic insulin sensitivity and the *DUSP8* variant was driven by a reduced insulin-induced suppression of hypothalamic CBF levels in men (**Figure 7D**; p=0.0131; p=0.0054, adjusted for age, BMI) but not women (**Figure 7E**; p=0.9006; p=0.9737, adjusted for age, BMI) carrying the *DUSP8* SNP rs2334499 minor-allele (T/T).

CBF was further assessed in the hippocampus (**Figure 7F**) as second insulin-sensitive and glucoregulatory brain region (31). We chose the hippocampus due to our recent work that revealed a smaller hippocampus size in Dusp8 KO mice, and reduced volumes of the hippocampal subregions subiculum and CA4 in humans carrying the risk variant rs2334499:C>T (16). We did not observe any differences in hippocampal CBF in response to intranasal insulin between the major, heterozygous or minor allele carriers regardless of their sex (**Figure 7G-I)**. Finally, whole-body insulin sensitivity was assessed by an oral glucose tolerance test (OGTT), but no correlation of the OGTT-derived insulin sensitivity index with the *DUSP8* SNP rs2334499 in these volunteers was found (p=0.7, adjusted for sex; p=0.9, adjusted for sex, age, BMI) (**Supplemental Table 3**). Similarly, plasma cortisol levels

were assessed but no difference between rs2334499 genotypes regardless of sex was found (**Supplemental Table 3**). Taken together, these findings from murine and human studies indicate that Dusp8 plays a role specifically in hypothalamic insulin sensitivity.

Discussion

We here describe a functional role for the GWAS target *DUSP8* in the hypothalamic regulation of glucose homeostasis. *DUSP8* was identified as potential novel diabetes type 2 risk gene in GWAS (9) and meta-analyses coalescing GWAS cohorts (32). In a small but well characterized cohort, we were able to show that homozygous male carriers of the minor frequency risk allele for *DUSP8* have impaired hypothalamic insulin sensitivity. We further showed increased *DUSP8* mRNA levels in the infundibular nucleus of T2D subjects. Murine studies further revealed systemic glucose intolerance and insulin resistance in male Dusp8 loss-of-function models exposed to HFD. Mechanistically, loss of the phosphatase Dusp8 deficiency was linked with Jnk hyper-activation in the mediobasal hypothalamus, leading to diminished glucocorticoid receptor activity, an impairment of HPA axis feedback and aggravation of systemic glucose tolerance due to basal hypercorticosteronemia driven by CRH neurons. Overall, our findings demonstrate a regulatory role of Dusp8 in hypothalamic inflammation, HPA axis reactivity and insulin sensitivity.

Collectively, our experiments revealed sex-specific effects on insulin sensitivity in mice and humans that were only present in male but not female subjects. This is in line with a previous report (9) where the association of the analyzed *DUSP8* SNP rs2334499 with T2D was also limited to male subjects. Reasons for the sex-specificity remain elusive, but the absence of effects on glucocorticoid action or hypothalamic inflammation in female Dusp8 KO mice may entail direct effects of sex-hormones such as estradiol (33) on HPA axis circuitry or peripheral glucoregulatory organs. Overall, our findings resonate with the emerging consensus that sex as a biological variable has to be a special focus in murine models and human studies. Another sex-related but entirely different phenomenon is the observation of the initial GWAS study showing that the T2D risk associated with rs2334499 was only inherited with the paternal allele (8). Such parent-of-origin information for the alleles was unfortunately not available in our cohort of volunteers. However, not including the family data in our analyses most likely lead us to underestimate the effect sizes of the detected association as we pooled the paternally inherited allele carrying the increased diabetes risk with the maternally inherited allele. The *DUSP8* SNP rs2334499 itself falls within close proximity of imprinted genes, but the region harboring it was reported to not be imprinted in human tissues or in mice (35), which was confirmed by clear biallelic expression for *DUSP8* in humans (11). Consistent with this, we did not observe a

phenotype in HFD-fed heterozygous Dusp8 KO males regardless of whether the mutated allele was inherited from the sire or dam.

Hypothalamic inflammation has been linked to impaired glucose metabolism and insulin sensitivity in obesity experimental models (34-36) and in humans (37). Acute hypothalamic inflammation is induced by long-chain saturated fatty acids that accumulate in the hypothalamus after crossing the blood brain barrier (35), where they activate pathways such as IKKβ/NFκB (38) to ultimately enhance the expressions of pro-inflammatory genes in the hypothalamus (28, 35), as observed in our Dusp8 KO model. Our finding of exacerbated hypothalamic Jnk activation, hypothalamic inflammation and an impairment of systemic glucose homeostasis in HFD-fed Dusp8 KO mice is moreover consistent with earlier reports that linked HFD-induced activation of Jnk signaling with both hypothalamic inflammation (28) and impaired glucose metabolism (25). Our hypothesis of a Jnk driven phenotype is further supported by a recent report on the restoration of hypothalamic insulin action after the pharmacological inhibition of reactive Jnk (39).

Mechanistically, our data suggest that hypothalamic Jnk hyperactivation due to Dusp8 ablation causes an impairment of GR activity (22) and aberrant negative HPA axis feedback, which ultimately drives excessive glucocorticoid secretion. The latter is a well-known risk factor for T2D (14, 40) that perturbs hepatic gluconeogenesis and glycogen storage as well as glucose uptake in skeletal muscle and white adipose tissue (41). We observed impaired glucose homeostasis due to elevated basal corticosterone levels and aberrant hepatic expression profiles of glucoregulatory enzymes in global HFD-fed Dusp8 KO males. Moreover, we found hyperactivation of Jnk signaling in the ARC of both global Dusp8 KO and Dusp8$^{CRH\text{-}Cre}$ KO male mice. This finding appears paradoxical, as it suggests that a Jnk-mediated impairment of the negative HPA axis feedback control in Dusp8 KO mice involves CRH neurons located (with their cell bodies) in the paraventricular nucleus (PVN), but originates in the ARC. Our data are nonetheless consistent with an earlier report that assessed the GR-mediated feedback inhibition of corticosterone on CRH release from PVN neurons (42). Specifically, when a GR antagonist was injected into the PVN where the CRH neurons were located, unperturbed feedback inhibition on adrenal corticosterone production was observed. In contrast, injection of the GR antagonist into the ARC disrupted the negative feedback, indicated by persistently increased circulating corticosterone levels (42). At present, we can only speculate on the nature of this effect.

Multiple studies have established dense communication between both areas, and ARC-specific AgRP neurons were shown to require hormonal input from CRH neurons (via CRFR1 receptor activation) to adapt to environmental challenges (20). Ablation of Dusp8 from AgRP neurons was however without effect on energy and glucose metabolism. Alternatively, Dusp8-positive CRH neuronal processes located within the ARC and close to the median eminence may be susceptible to the effects of circulating corticosterone, a process perturbed locally in the ARC by hypothalamic inflammation. The phenomenon, i.e. impaired negative feedback of corticosterone on CRH release that is driven by the ARC, remains unresolved and is a limitation of our study that warrants future investigation.

Impaired HPA axis feedback inhibition in Dusp8 KO mice subjected to a Dex/CRH test, and the rescue of glucose intolerance in Dusp8 KO mice subjected to AAV-mediated Dusp8 overexpression in the mediobasal hypothalamus, nonetheless corroborates an important role for hypothalamic Dusp8 as a regulator of Jnk1-driven feedback inhibition of the HPA axis. Our finding of reduced sympathetic outflow in HFD-fed Dusp8 KO mice was further in accordance to studies in humans showing glucocorticoid-induced sympatho-inhibition (12, 13). Similarly, when patients with metabolic syndrome were stratified for insulin-resistance and challenged with a glucose bolus, they showed blunted sympathetic activity and reduced NE clearance from plasma compared to insulin sensitive patients with metabolic syndrome (43). Taken together, these data indicate that impaired glucocorticoid feedback in the hypothalamus, and the reduction in SNS tone contribute to the insulin resistance observed in our Dusp8 KO model.

In line with the central role for Jnk1 in the regulation of glucose metabolism (24, 25), co-deletion of Jnk1 normalized glucose tolerance and hypercorticosteronemia in HFD-fed Dusp8 KO mice. However, significant MAPK cross-talk (2) and Dusp8 phosphatase activity towards other Jnk isoforms (44) or p38 (11) have been reported. Accordingly, our data cannot fully exclude that MAPK other than Jnk1 play a role in the etiology of the glucose intolerance phenotype of HFD-fed Dusp8 KO males. Similarly, our findings do not exclude a role for Dusp8 in hypothalamic subpopulations distinct from CRH neurons, in other brain areas, or in peripheral tissues. Moreover, the ablation of Dusp8 may exert distinct effects in each of these subpopulations, areas or tissues and future studies are thus warranted to address these current limitations. Based on our data on Dusp8 KO, p38AF DN double mutants, we can already exclude a potential role for p38. Similarly, our data do not point toward ERK as potential

mediator of impaired glucose metabolism in HFD-fed Dusp8 KO males as hypothalamic ERK was shown to be prominently involved in the control of food intake, body weight, and thermogenic sympathetic outflow, but not in the regulation of glucose homeostasis (45). Collectively, our data support a model whereby hypothalamic Dusp8 becomes activated upon diet-induced obesity to control and change the magnitude of hypothalamic Jnk activity. Dusp8 thus serves as gatekeeper against the deleterious effects that chronically increased Jnk signaling has on the regulation of energy and glucose homeostasis (2, 24).

Hypothalamic insulin resistance was present in HFD-fed Dusp8 KO mice and human carriers of the *DUSP8* T2D risk allele. Stimulating brain insulin action by intranasal insulin improves whole-body insulin sensitivity in healthy human men, but not in obese patients with hypothalamic insulin resistance (46, 47). We have previously linked hypothalamic insulin responsiveness with pancreatic insulin secretion (48) and revealed an elevated second phase insulin secretion in humans upon hypothalamic insulin action (49). Similarly, we showed that hypothalamic insulin action was linked with suppressed endogenous glucose production and elevated glucose uptake (47) as well as alterations in parasympathetic output (50). Studies in young men further linked intranasal insulin administration with attenuated HPA axis activity (51), but molecular underpinnings for this central action of insulin remained unresolved (52). Future studies are thus warranted to clarify the impact of central insulin, and rs2334499 polymorphisms, on the HPA axis of human subjects with or without T2D.

Overall, our results indicate a multi-systemic process whereby hypothalamic insulin resistance, combined with deregulated HPA axis reactivity, autonomous nervous system activity and corticosterone release, exacerbates the detrimental effects of chronic high-fat diet feeding on systemic glucose homeostasis in male Dusp8 deficient mice via increased hypothalamic Jnk activity. Importantly, these effects appear to translate into the human situation, where T2D subjects had increased *DUSP8* expression in the infundibular nucleus and male carriers of T2D risk variant rs2334499 displayed impaired hypothalamic insulin sensitivity. Replication of our human finding would be central, but our findings already extend previous GWAS studies that suggest Dusp8 as T2D risk variant. In sum, we reveal that hypothalamic Dusp8 is a crucial gatekeeper for the Jnk-dependent control of systemic glucose homeostasis.

Material and Methods

Animals: C57BL/6J mice were obtained from Janvier (Le Genest-Saint-Isle, France) and Lepob (JAX stock #000632), Jnk1 KO (JAX stock #004319), and p38AF DN (JAX stock #012736) mice were obtained from Jackson Laboratory (Bar Harbor, ME, USA). Dusp8 KO mice were derived from breeding of Dusp8 heterozygous mice generously donated by the Molkentin laboratory (21) with pure C57BL/6J background. Jnk1-Dusp8 dKO mice were derived from breedings of Dusp8 heterozygous mice with Jnk1 heterozygous mice that had been crossed back to B6/J background. Dusp8 KO, $p38^{AF}$ DN mice were generated by breeding mice heterozygous for the dominant-negative allele of p38 (p38(AF)) with Dusp8 heterozygous mice.

The Dusp8 conditional knockout line was generated from the Dusp8tm1a(EUCOMM)Hmgu embryonic stem (ES) cell clone HEPD0822-2-A10 (European Mammalian Mutant Cell Repository) as detailed in the Supplemental Methods. Conditional Dusp8 ($Dusp8^{fl/fl}$) mice were crossed to CRH-Cre (JAX stock #012704), AgRP-Cre (JAX stock #012899) or POMC-Cre (JAX stock # 005965) mice, respectively.

Mice with an age of 8 to 10 weeks were either maintained on chow (5.6% fat, LM-485, Harlan Teklad or Altromin 1314) or switched to HFD (45% kcal fat; Research Diets Inc., New Brunswick, NJ, USA) for up to 30 weeks. All WT and KO mice used in our studies were littermates. Mice were group housed on a 12:12 h light-dark cycle at 22°C with free access to food and water, unless indicated otherwise. Mice were distributed into experimental groups based on their body weights to assure an equal distribution of body weights at the beginning of the study. In vivo experiments were performed without blinding of the investigators. All studies were based on power analyses to assure adequate sample sizes, and approved by the State of Bavaria, Germany, or by the Institutional Animal Care and Use Committee of the University of Cincinnati.

Body composition analysis: Fat mass and lean mass were measured via Nuclear Magnetic Resonance (NMR) technology (EchoMRI, Houston, TX, USA).

Glucose, insulin and pyruvate tolerance tests (GTT/ITT/PTT): For the GTT and ITT, mice were subjected to 6 h of fasting one hour after the onset of the light phase. For the PTT, mice were fasted

overnight for 16 hours. Subsequently, HFD-fed mice were injected intraperitoneally with 1.5 g glucose/kg body weight (BW) for the GTT, 0.75 or 1.0 U insulin/kg BW (0.09 U/ml; Humolog Pen, Eli Lilly, Indianapolis, IN, USA) for the ITT and 0.75 g pyruvate/kg BW for the PTT. Chow-fed mice received 2.0 g glucose/kg BW for the GTT and 0.75 U insulin/kg BW for the ITT. Tail blood glucose levels (mg/dl) were measured with a handheld glucometer (TheraSense Freestyle) before (0 min) and at 15, 30, 60 and 120 min after injection. For the glucose-stimulated insulin secretion test (GSIST), 1.5 mg glucose/kg BW was injected intravenously in 6 hours fasted HFD-fed mice. Tail blood for insulin measurements was collected at 0, 1, 5, 10 and 60 min after injection.

Adeno-associated virus (AAV) infusion in mice: Custom-made AAVs (serotype AAV5) with full-length murine Dusp8 cDNA under the control of a CMV promoter or an AAV with CMV-GFP as control (pAAV5-CMV-Dusp8 vs. pAAV5-CMV-eGFP; 2×10^9 viral genome particles/ml; Sirion Biotechnology, Martinsried, Germany) were injected bilateraly into the mediobasal hypothalamus of single-housed, DIO WT and Dusp8 KO littermates (6-months-old) using a motorized stereotaxic system from Neurostar as detailed in the Supplemental Methods.

Acute insulin challenge: To assess biochemical responses to insulin stimulation, insulin was administered intraperitoneally at a dose of 3 U/kg BW in age-matched DIO WT and Dusp8 KO littermates. Control mice received vehicle instead. Mice were sacrificed 8 min after insulin administration by cervical dislocation. Hypothalami were collected to measure signal transduction markers by Western blotting.

Catecholamine turnover rate determination: Catecholamine turnover was measured on the basis of the decline in tissue NE content after the inhibition of catecholamine biosynthesis with a-methyl-DL-tyrosine methyl ester hydrochloride (α-MPT, #M3281, Sigma-Aldrich) as described previously (53) and in the Supplemental Methods.

Dex/CRH test: In the combined Dex/CRH test (17), the corticosterone secretion of Dusp8 KO and WT mice was monitored in response to a pharmacological suppression of adrenocortical activity with

dexamethasone (0.05 mg/kg BW) and a subsequent stimulation with corticotropin-releasing hormone (0.15 mg/kg BW) as detailed in the Supplemental Methods.

Metyrapone injections: Age matched DIO WT and Dusp8 KO littermates (7-months-old) received daily intraperitoneal injections of 100 mg/kg BW metyrapone (Cat # M2696, Sigma-Aldrich) for 14 days that were shown to reduce endogenous corticosterone production (18).

Immunohistochemistry and Immunofluorescence: PFA-fixed brains were processed for cryo-sectioning followed by immunohistochemical and immunofluorescent stainings in the free floating approach as detailed in the Supplemental Methods.

In situ hybridization: Coronal hypothalamic sections (16 µm) were cut on a cryostat and immediately stored at -80°C until hybridization. Sense and anti-sense probes were generated from the Dusp8 cDNA sequence using a digoxigenin (DIG) RNA labeling kit (Roche). The hybridization procedure is described in detail in the Supplemental Methods.

Blood chemistry: Blood was collected in EDTA-containing centrifuge tubes and centrifuged at 4°C and 2000xg for 10 min. Plasma triglycerides, cholesterol and non-esterified fatty acids (NEFA) were measured by commercial enzymatic assay kits (Wako Chemicals, Neuss, Germany). Insulin and leptin were measured by ultrasensitive murine insulin and murine leptin ELISA kits (Merck Millipore, Darmstadt, Germany). Plasma corticosterone levels were measured by radioimmunoassay (MP Biomedicals Inc, USA; sensitivity 6.25 ng/ml) or corticosterone ELISA kit (Abor Assays, Ann Arbor, MI, USA). All assays were performed according to the manufacturer's instructions.

Hepatic triglyceride and glycogen content measurements: Hepatic triglyceride content was determined by using a triglyceride assay kit (Wako Chemicals, Neuss, Germany) as described. Hepatic glycogen content was measured by the enzymatic starch analysis assay (R-Biopharm AG, Darmstadt, Deutschland) according to the manufacturer's instructions.

Cell culture: Hek293 cells (Leibniz Institute DSMZ, Braunschweig, Germany, RRID:CVCL_0045) were grown in Dulbeco's modied Eagle's medium (DMEM) supplemented with 10% fetal calf serum and 1% pencillin/streptomycin. Cell lines were tested for mycoplasma contamination after thawing and every other month in culture. Transient transfections were performed using FuGene reagent from Promega (Madison, WI) and plasmids for pCMV6 (#PS100020, OriGene Technologies, Rockville, MD, USA) or pCMV6-Dusp8 (#MR209863, OriGene) and pcDNA3.1-hGR (54) as indicated in serum-free medium. Stimulation experiments were performed 48h post transfection.

GR luciferase assay: For luciferase assays, Hek293 cells were seeded into 96-well plates and grown overnight to 70–80% confluence. Cells were then transiently transfected with pGL4-Per1 (54), pRL-TK (#E2241, Promega, Madison, WI) and pCMV6 or pCMV6-Dusp8 plasmids. 24 hours past transfection, cells where indicated were pretreated with anisomycin (100 nM) overnight and then stimulated with Dex (100 nM) for 5 hours. All samples were run in triplicate. Luciferase activity was measured using a microplate luminometer (PHERAstar, BMG Labtech, Germany) and the Dual-Glo® Luciferase Assay System (Promega), according to the instruction from the manufacturer.

Protein extraction and Western blotting analysis: Hek293 cells and murine tissues were processed for protein extraction, concentration determination and Western blot analysis as detailed in the Supplemental Methods.

Microarray analysis of laser-capture-microdissected arcuate nucleus: Perfused and sucrose-equilibrated brains of global Dusp8 WT and KO males were cut coronally followed by laser capture microdissection of the arcuate nucleus. Subsequently, RNA was isolated from the arcuate nuclei and gene expression was analyzed by microarray. Details are given in the Supplemental Methods.

RNA isolation and qPCR analysis: RNA was isolated from flash-frozen murine tissues and post-mortem formalin-fixed, paraffin-embedded (FFPE) human brain tissue with commercially available kits and reverse transcribed into cDNA followed by gene expression analysis as detailed in the Supplemental Methods.

Human data: *DUSP8* expression in the infundibular nucleus was assessed in post-mortem hypothalamic tissues of 11 T2D and 12 non-T2D controls subjects obtained from the Netherlands Brain Bank (29). Regional brain insulin sensitivity was assessed in a group of 47 healthy participants of the ongoing TUF study (55) (**Supplemental Table 3**), using an established protocol that combines the measurement of cerebral blood flow by functional MRI with the delivery of 160 U of insulin as nasal spray as described previously (30). Blood flow for the hypothalamic and hippocampal region of interest (ROI) was extracted and associations with the *DUSP8* SNP rs2334499 (major allele (C/C), heterozygous (C/T), minor allele (T/T)) were tested by multiple linear regression analyses with adjustment for age.

Statistical analyses: In vivo measurements were taken from distinct samples and in vitro measurements were performed in at least 3 independent biological replicates. For animal experiments, we performed power analysis with the assumption of normality. Statistical significant outliers were identified by Grubb's test. All statistical analyses (except microarray analysis) were performed using GraphPad Prism, SPSS, SAS or JMP. Two groups were compared by using two-tailed unpaired Student's *t*-test or the non-parametric Wilcoxon rank-sum test. Multiple comparison analyses were performed by using one- or two-way ANOVAs followed by Tuckey or Bonferroni post hoc tests. Combined indirect calorimetry measurements were assessed by Analysis of Co-Variance (ANCOVA), using body weight as covariate. *p*-values lower than 0.05 were considered significant. Results are presented as scatter dot plots, as means ± s.e.m.or as box-and-whisker-plots (median, 25th and 75th quartile, whiskers 5-95 percentiles).

Data availability: The microarray data has been submitted to the GEO database at NCBI (GSE112688: https://www.ncbi.nlm.nih.gov/geo/query/acc.cgi?acc=GSE112688). The mass spectrometry proteomics data have been deposited to the ProteomeXchange Consortium via the PRIDE (56) partner repository with the dataset identifier PXD019451. All other data generated or analyzed during this study are available within the paper and its supplementary information file.

Study approval: All animal studies were approved by the State of Bavaria, Germany, or by the Institutional Animal Care and Use Committee of the University of Cincinnati. Autopsies to obtain hypothalamic tissue samples post-mortem were approved by the Medical Ethic Committee of the VU Medical Center, The Netherlands. All human subjects of the TUF study provided informed written consent prior to the inclusion in the study and the local ethics committee of the University of Tuebingen approved the protocol.

Limitations of human data: A replication of our human finding of reduced CBF in rs2334499 minor allele carriers would be central. As the effect size for the association with hypothalamic insulin sensitivity is much larger than the effect size of the association with diabetes risk, a considerably smaller cohort than the initial discovery cohorts for diabetes risk would be sufficient for such a replication approach. Unfortunately, we are not aware of any other human cohort with quantification of hypothalamic insulin sensitivity and genetic information. Future replication is nonetheless warranted to substantiate our findings.

Author Contributions

SCS, DGK, KP, PB, EVB, LH, FG, RJ, JC, SM, MW, TM, KS, WW, RN, JDM, SL and PTP performed in vivo experiments in mice. SCS, DGK and PTP designed, performed and analyzed the AAV infusion study. JC, SM, SL, MW, SCS and JR planned, performed and analyzed the in vivo delineation of insulin resistance. SCS, SL, JN and KWS designed, performed and analyzed the aMPT study. MVS, PTP and SCS designed, performed and analyzed the dexamethasone suppression test and the metyrapone study. FS and NK performed the phospho-proteome analysis. MI, MHA and JB performed and analyzed the microarray study. SCS, DGK and CXY conducted immunohistochemical stainings. RN performed in situ hybridizations. SCS, EVB and HS performed qPCRs and Western Blot analyzes. SCS, FCS and CXY designed, performed and analyzed the gene expression in post-mortem humans brain tissue. SK, HUH and MH designed, performed and analyzed the fMRI study and plasma measurements of humans from the TUF cohort. SCS, MVS, SL, MH, MHT and PTP designed experiments, analyzed and interpreted the results. SCS, MH, MVS, SL, MHT and PTP prepared the manuscript. SCS, MHT and PTP developed the conceptual framework of this study.

Competing Interests

Dr. Matthias Tschöp is a member of the scientific advisory board of ERX Pharmaceuticals, Inc., Cambridge, MA. He was a member of the Research Cluster Advisory Panel (ReCAP) of the Novo Nordisk Foundation between 2017-2019. He attended a scientific advisory board meeting of the Novo Nordisk Foundation Center for Basic Metabolic Research in 2016. He received funding for his research projects by Novo Nordisk (2016-2020) and Sanofi-Aventis (2012-2019). He was a consultant for Bionorica SE (2013-2017), Menarini Ricerche S.p.A. (2016), and Bayer Pharma AG Berlin (2016). As former Director of the Helmholtz Diabetes Center and the Institute for Diabetes and Obesity at Helmholtz Zentrum München (2011-2018) and since 2018 as CEO of Helmholtz Zentrum München he has been responsible for collaborations with a multitude of companies and institutions, worldwide. In this capacity, he discussed potential projects with and has signed/signs contracts for his institute(s) and for the staff for research funding and/or collaborations with industry and academia, worldwide, including but not limited to pharmaceutical corporations like Boehringer Ingelheim, Eli Lilly, Novo Nordisk, Medigene, Arbormed, BioSyngen and others. In this role, he was/is further responsible for

commercial technology transfer activities of his institute(s), including diabetes related patent portfolios of Helmholtz Zentrum München, e.g. WO/2016/188932 A2 or WO/2017/194499 A1. Dr. Tschöp confirms that to the best of his knowledge none of the above funding sources were involved in the preparation of this paper.

Acknowledgements

We thank Sarah Jelinek, Marlene Kilian, Verónica Casquero, Anke Bettenbrock, Emilija Malogajski, Daniel Brandt and Bea Deiml for their skillful technical assistance. We are most grateful to Aurélie Joly Amado for excellent advice on the norephinephrine turnover studies. Jeff Molkentin very kindly provided the global Dusp8 KO model. Andreas Peter kindly performed the genotyping of the TUF cohort. Henriette Uhlenhaut very kindly provided the hGR plasmid and the pGL4-Per1 luciferase assay plasmid.

This work was supported in part by the Helmholtz Portfolio Program "Metabolic Dysfunction" (MHT), by the Alexander von Humboldt Foundation (MHT), by the Helmholtz Alliance ICEMED-Imaging and Curing Environmental Metabolic Diseases (SCS, MHT, HUH), by the German Center for Diabetes Research (DZD; SCS, PP, MH, MHA), by the Helmholtz-Israel-Cooperation in Personalized Medicine (PP), by the Helmholtz Initiative for Personalized Medicine (iMed; MHT), by the Helmholtz Alliance 'Aging and Metabolic Programming, AMPro' (JB, NK), by the Emmy-Noether DFG 'KR5166/1-1' (NK), by German Federal Ministry of Education and Research '01KX1012' (MHA) and through the Initiative and Networking Fund of the Helmholtz Association.

References

1. Hotamisligil GS, Shargill NS, and Spiegelman BM. Adipose expression of tumor necrosis factor-alpha: direct role in obesity-linked insulin resistance. *Science.* 1993;259(5091):87-91.
2. Kyriakis JM, and Avruch J. Mammalian MAPK signal transduction pathways activated by stress and inflammation: a 10-year update. *Physiol Rev.* 2012;92(2):689-737.
3. Kondoh K, and Nishida E. Regulation of MAP kinases by MAP kinase phosphatases. *Biochim Biophys Acta.* 2007;1773(8):1227-37.
4. Seternes OM, Kidger AM, and Keyse SM. Dual-specificity MAP kinase phosphatases in health and disease. *Biochim Biophys Acta Mol Cell Res.* 2019;1866(1):124-43.
5. Farooq A, and Zhou MM. Structure and regulation of MAPK phosphatases. *Cell Signal.* 2004;16(7):769-79.
6. Choi HR, Kim WK, Kim EY, Han BS, Min JK, Chi SW, Park SG, Bae KH, and Lee SC. Dual-specificity phosphatase 10 controls brown adipocyte differentiation by modulating the phosphorylation of p38 mitogen-activated protein kinase. *PLoS One.* 2013;8(8):e72340.
7. Ferguson BS, Nam H, and Morrison RF. Dual-specificity phosphatases regulate mitogen-activated protein kinase signaling in adipocytes in response to inflammatory stress. *Cell Signal.* 2019;53(234-45.
8. Kong A, Steinthorsdottir V, Masson G, Thorleifsson G, Sulem P, Besenbacher S, Jonasdottir A, Sigurdsson A, Kristinsson KT, Jonasdottir A, et al. Parental origin of sequence variants associated with complex diseases. *Nature.* 2009;462(7275):868-74.
9. Morris AP, Voight BF, Teslovich TM, Ferreira T, Segre AV, Steinthorsdottir V, Strawbridge RJ, Khan H, Grallert H, Mahajan A, et al. Large-scale association analysis provides insights into the genetic architecture and pathophysiology of type 2 diabetes. *Nat Genet.* 2012;44(9):981-90.
10. Martell KJ, Seasholtz AF, Kwak SP, Clemens KK, and Dixon JE. hVH-5: a protein tyrosine phosphatase abundant in brain that inactivates mitogen-activated protein kinase. *J Neurochem.* 1995;65(4):1823-33.
11. Muda M, Theodosiou A, Rodrigues N, Boschert U, Camps M, Gillieron C, Davies K, Ashworth A, and Arkinstall S. The dual specificity phosphatases M3/6 and MKP-3 are highly selective for inactivation of distinct mitogen-activated protein kinases. *J Biol Chem.* 1996;271(44):27205-8.
12. Golczynska A, Lenders JW, and Goldstein DS. Glucocorticoid-induced sympathoinhibition in humans. *Clin Pharmacol Ther.* 1995;58(1):90-8.
13. Cameron OG, Starkman MN, and Schteingart DE. The effect of elevated systemic cortisol levels on plasma catecholamines in Cushing's syndrome patients with and without depressed mood. *J Psychiatr Res.* 1995;29(5):347-60.
14. Tomlinson JW, Finney J, Gay C, Hughes BA, Hughes SV, and Stewart PM. Impaired glucose tolerance and insulin resistance are associated with increased adipose 11beta-hydroxysteroid dehydrogenase type 1 expression and elevated hepatic 5alpha-reductase activity. *Diabetes.* 2008;57(10):2652-60.
15. Joly-Amado A, Denis RG, Castel J, Lacombe A, Cansell C, Rouch C, Kassis N, Dairou J, Cani PD, Ventura-Clapier R, et al. Hypothalamic AgRP-neurons control peripheral substrate utilization and nutrient partitioning. *EMBO J.* 2012;31(22):4276-88.
16. Baumann P, Schriever SC, Kullmann S, Zimprich A, Feuchtinger A, Amarie O, Peter A, Walch A, Gailus-Durner V, Fuchs H, et al. Dusp8 affects hippocampal size and behavior in mice and humans. *Sci Rep.* 2019;9(1):19483.

17. Touma C, Gassen NC, Herrmann L, Cheung-Flynn J, Bull DR, Ionescu IA, Heinzmann JM, Knapman A, Siebertz A, Depping AM, et al. FK506 binding protein 5 shapes stress responsiveness: modulation of neuroendocrine reactivity and coping behavior. *Biol Psychiatry.* 2011;70(10):928-36.
18. Takeshita N, Yoshino T, and Mutoh S. Possible involvement of corticosterone in bone loss of genetically diabetic db/db mice. *Horm Metab Res.* 2000;32(4):147-51.
19. Belgardt BF, Okamura T, and Bruning JC. Hormone and glucose signalling in POMC and AgRP neurons. *J Physiol.* 2009;587(Pt 22):5305-14.
20. Kuperman Y, Weiss M, Dine J, Staikin K, Golani O, Ramot A, Nahum T, Kuhne C, Shemesh Y, Wurst W, et al. CRFR1 in AgRP Neurons Modulates Sympathetic Nervous System Activity to Adapt to Cold Stress and Fasting. *Cell Metab.* 2016;23(6):1185-99.
21. Liu R, van Berlo JH, York AJ, Vagnozzi RJ, Maillet M, and Molkentin JD. DUSP8 Regulates Cardiac Ventricular Remodeling by Altering ERK1/2 Signaling. *Circ Res.* 2016;119(2):249-60.
22. Rogatsky I, Logan SK, and Garabedian MJ. Antagonism of glucocorticoid receptor transcriptional activation by the c-Jun N-terminal kinase. *Proc Natl Acad Sci U S A.* 1998;95(5):2050-5.
23. Campbell JN, Macosko EZ, Fenselau H, Pers TH, Lyubetskaya A, Tenen D, Goldman M, Verstegen AM, Resch JM, McCarroll SA, et al. A molecular census of arcuate hypothalamus and median eminence cell types. *Nat Neurosci.* 2017;20(3):484-96.
24. Hirosumi J, Tuncman G, Chang L, Gorgun CZ, Uysal KT, Maeda K, Karin M, and Hotamisligil GS. A central role for JNK in obesity and insulin resistance. *Nature.* 2002;420(6913):333-6.
25. Belgardt BF, Mauer J, Wunderlich FT, Ernst MB, Pal M, Spohn G, Bronneke HS, Brodesser S, Hampel B, Schauss AC, et al. Hypothalamic and pituitary c-Jun N-terminal kinase 1 signaling coordinately regulates glucose metabolism. *Proc Natl Acad Sci U S A.* 2010;107(13):6028-33.
26. Wong ES, Le Guezennec X, Demidov ON, Marshall NT, Wang ST, Krishnamurthy J, Sharpless NE, Dunn NR, and Bulavin DV. p38MAPK controls expression of multiple cell cycle inhibitors and islet proliferation with advancing age. *Dev Cell.* 2009;17(1):142-9.
27. Aguirre V, Uchida T, Yenush L, Davis R, and White MF. The c-Jun NH(2)-terminal kinase promotes insulin resistance during association with insulin receptor substrate-1 and phosphorylation of Ser(307). *J Biol Chem.* 2000;275(12):9047-54.
28. De Souza CT, Araujo EP, Bordin S, Ashimine R, Zollner RL, Boschero AC, Saad MJ, and Velloso LA. Consumption of a fat-rich diet activates a proinflammatory response and induces insulin resistance in the hypothalamus. *Endocrinology.* 2005;146(10):4192-9.
29. Hogenboom R, Kalsbeek MJ, Korpel NL, de Goede P, Koenen M, Buijs RM, Romijn JA, Swaab DF, Kalsbeek A, and Yi CX. Loss of arginine vasopressin- and vasoactive intestinal polypeptide-containing neurons and glial cells in the suprachiasmatic nucleus of individuals with type 2 diabetes. *Diabetologia.* 2019;62(11):2088-93.
30. Kullmann S, Heni M, Veit R, Scheffler K, Machann J, Haring HU, Fritsche A, and Preissl H. Selective insulin resistance in homeostatic and cognitive control brain areas in overweight and obese adults. *Diabetes Care.* 2015;38(6):1044-50.
31. Soto M, Cai W, Konishi M, and Kahn CR. Insulin signaling in the hippocampus and amygdala regulates metabolism and neurobehavior. *Proc Natl Acad Sci U S A.* 2019;116(13):6379-84.
32. Billings LK, and Florez JC. The genetics of type 2 diabetes: what have we learned from GWAS? *Ann N Y Acad Sci.* 2010;1212(59-77.

33. Hong J, Stubbins RE, Smith RR, Harvey AE, and Nunez NP. Differential susceptibility to obesity between male, female and ovariectomized female mice. *Nutr J.* 2009;8(11.

34. Jais A, and Bruning JC. Hypothalamic inflammation in obesity and metabolic disease. *J Clin Invest.* 2017;127(1):24-32.

35. Posey KA, Clegg DJ, Printz RL, Byun J, Morton GJ, Vivekanandan-Giri A, Pennathur S, Baskin DG, Heinecke JW, Woods SC, et al. Hypothalamic proinflammatory lipid accumulation, inflammation, and insulin resistance in rats fed a high-fat diet. *Am J Physiol Endocrinol Metab.* 2009;296(5):E1003-12.

36. Romanatto T, Cesquini M, Amaral ME, Roman EA, Moraes JC, Torsoni MA, Cruz-Neto AP, and Velloso LA. TNF-alpha acts in the hypothalamus inhibiting food intake and increasing the respiratory quotient--effects on leptin and insulin signaling pathways. *Peptides.* 2007;28(5):1050-8.

37. Kreutzer C, Peters S, Schulte DM, Fangmann D, Turk K, Wolff S, van Eimeren T, Ahrens M, Beckmann J, Schafmayer C, et al. Hypothalamic Inflammation in Human Obesity Is Mediated by Environmental and Genetic Factors. *Diabetes.* 2017;66(9):2407-15.

38. Kleinridders A, Schenten D, Konner AC, Belgardt BF, Mauer J, Okamura T, Wunderlich FT, Medzhitov R, and Bruning JC. MyD88 signaling in the CNS is required for development of fatty acid-induced leptin resistance and diet-induced obesity. *Cell Metab.* 2009;10(4):249-59.

39. Benzler J, Ganjam GK, Legler K, Stohr S, Kruger M, Steger J, and Tups A. Acute inhibition of central c-Jun N-terminal kinase restores hypothalamic insulin signalling and alleviates glucose intolerance in diabetic mice. *J Neuroendocrinol.* 2013;25(5):446-54.

40. Di Dalmazi G, Pagotto U, Pasquali R, and Vicennati V. Glucocorticoids and type 2 diabetes: from physiology to pathology. *J Nutr Metab.* 2012;2012(525093.

41. de Guia RM, Rose AJ, and Herzig S. Glucocorticoid hormones and energy homeostasis. *Horm Mol Biol Clin Investig.* 2014;19(2):117-28.

42. Leon-Mercado L, Herrera Moro Chao D, Basualdo MD, Kawata M, Escobar C, and Buijs RM. The Arcuate Nucleus: A Site of Fast Negative Feedback for Corticosterone Secretion in Male Rats. *eNeuro.* 2017;4(1).

43. Straznicky NE, Lambert GW, Masuo K, Dawood T, Eikelis N, Nestel PJ, McGrane MT, Mariani JA, Socratous F, Chopra R, et al. Blunted sympathetic neural response to oral glucose in obese subjects with the insulin-resistant metabolic syndrome. *Am J Clin Nutr.* 2009;89(1):27-36.

44. Oehrl W, Cotsiki M, and Panayotou G. Differential regulation of M3/6 (DUSP8) signaling complexes in response to arsenite-induced oxidative stress. *Cell Signal.* 2013;25(2):429-38.

45. Rahmouni K, Sigmund CD, Haynes WG, and Mark AL. Hypothalamic ERK mediates the anorectic and thermogenic sympathetic effects of leptin. *Diabetes.* 2009;58(3):536-42.

46. Heni M, Kullmann S, Preissl H, Fritsche A, and Haring HU. Impaired insulin action in the human brain: causes and metabolic consequences. *Nat Rev Endocrinol.* 2015;11(12):701-11.

47. Heni M, Wagner R, Kullmann S, Gancheva S, Roden M, Peter A, Stefan N, Preissl H, Haring HU, and Fritsche A. Hypothalamic and Striatal Insulin Action Suppresses Endogenous Glucose Production and May Stimulate Glucose Uptake During Hyperinsulinemia in Lean but Not in Overweight Men. *Diabetes.* 2017;66(7):1797-806.

48. Kullmann S, Fritsche A, Wagner R, Schwab S, Haring HU, Preissl H, and Heni M. Hypothalamic insulin responsiveness is associated with pancreatic insulin secretion in humans. *Physiol Behav.* 2017;176(134-8.

49. Heni M, Wagner R, Willmann C, Jaghutriz BA, Vosseler A, Kubler C, Hund V, Scheffler K, Peter A, Haring HU, et al. Insulin action in the hypothalamus increases second phase insulin secretion in humans. *Neuroendocrinology.* 2019.

50. Heni M, Wagner R, Kullmann S, Veit R, Mat Husin H, Linder K, Benkendorff C, Peter A, Stefan N, Haring HU, et al. Central insulin administration improves whole-body insulin sensitivity via hypothalamus and parasympathetic outputs in men. *Diabetes.* 2014;63(12):4083-8.
51. Benedict C, Hallschmid M, Hatke A, Schultes B, Fehm HL, Born J, and Kern W. Intranasal insulin improves memory in humans. *Psychoneuroendocrinology.* 2004;29(10):1326-34.
52. Plum L, Schubert M, and Bruning JC. The role of insulin receptor signaling in the brain. *Trends Endocrinol Metab.* 2005;16(2):59-65.
53. Brodie BB, Costa E, Dlabac A, Neff NH, and Smookler HH. Application of steady state kinetics to the estimation of synthesis rate and turnover time of tissue catecholamines. *J Pharmacol Exp Ther.* 1966;154(3):493-8.
54. Uhlenhaut NH, Barish GD, Yu RT, Downes M, Karunasiri M, Liddle C, Schwalie P, Hubner N, and Evans RM. Insights into negative regulation by the glucocorticoid receptor from genome-wide profiling of inflammatory cistromes. *Mol Cell.* 2013;49(1):158-71.
55. Stumvoll M, Tschritter O, Fritsche A, Staiger H, Renn W, Weisser M, Machicao F, and Haring H. Association of the T-G polymorphism in adiponectin (exon 2) with obesity and insulin sensitivity: interaction with family history of type 2 diabetes. *Diabetes.* 2002;51(1):37-41.
56. Perez-Riverol Y, Csordas A, Bai J, Bernal-Llinares M, Hewapathirana S, Kundu DJ, Inuganti A, Griss J, Mayer G, Eisenacher M, et al. The PRIDE database and related tools and resources in 2019: improving support for quantification data. *Nucleic Acids Res.* 2019;47(D1):D442-D50.

Figure titles and legends

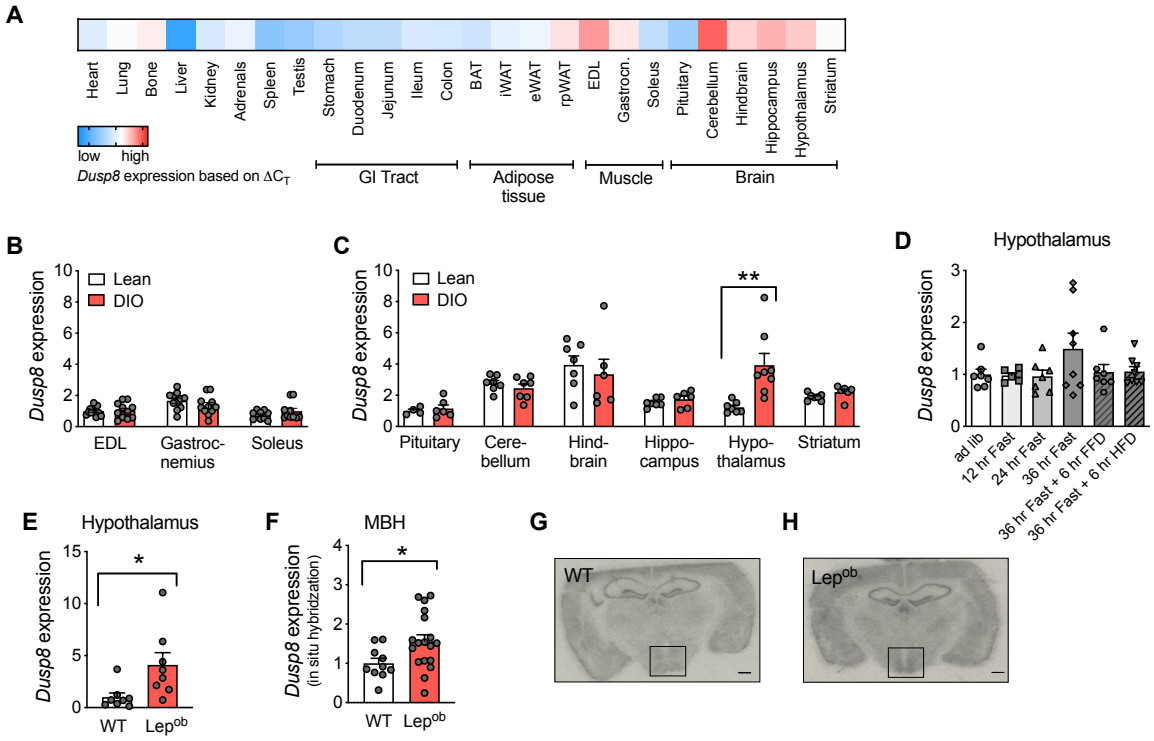

Figure 1: Hypothalamic *Dusp8* expression is regulated by body adiposity.

A) Tissue specific expression levels of *Dusp8* were assessed in lean C567Bl6J male mice (n=3) and are presented as ΔC_T values with low *Dusp8* expression in blue and high *Dusp8* expression in red. Regulation of *Dusp8* expression by adiposity was analyzed in lean vs. diet-induced obese (DIO) male mice for **B)** skeletal muscle [EDL (n=12 WT, n=11 KO), gastrocnemius (n=11 WT, n=12 KO), soleus (n=10 WT, n=12 KO)] and **C)** micro-dissected brain regions [pituitary (n=4 WT, n=6 KO), cerebellum (n=6 WT, n=6 KO), hindbrain (n=6 WT, n=5 KO), hippocampus (n=5 WT, n=6 KO), hypothalamus (n=6 WT, n=6 KO) and striatum (n=6 WT, n=5 KO) and is shown as ΔC_T values. **D)** Hypothalamic *Dusp8* mRNA expression in C57BL/6J mice that were subjected to 12 (n=6), 24 (n=7) or 36 (n=8) hours of fasting as well as refeeding for 6 hours with fat free (FFD, n=7) or high-fat (HFD, n=8) diet compared to ad lib control (n=7). **E)** Hypothalamic *Dusp8* mRNA levels in male *Lep^{ob}* vs. WT mice (n=8). **F)** Densitometric analysis of Dusp8 mRNA by *in situ* hybridization localized *Dusp8* expression to the MBH of male **G)** WT and **H)** *Lep^{ob}* mice (n=18) mice, representative pictures.

Data are shown as heatmap (A) or as scatter dot plots with means ± s.e.m. (B-F). Scale bar = 500 µm. *p<0.05 and **p<0.01; Student's t-test (B,C,E,F) or One-Way ANOVA (D).

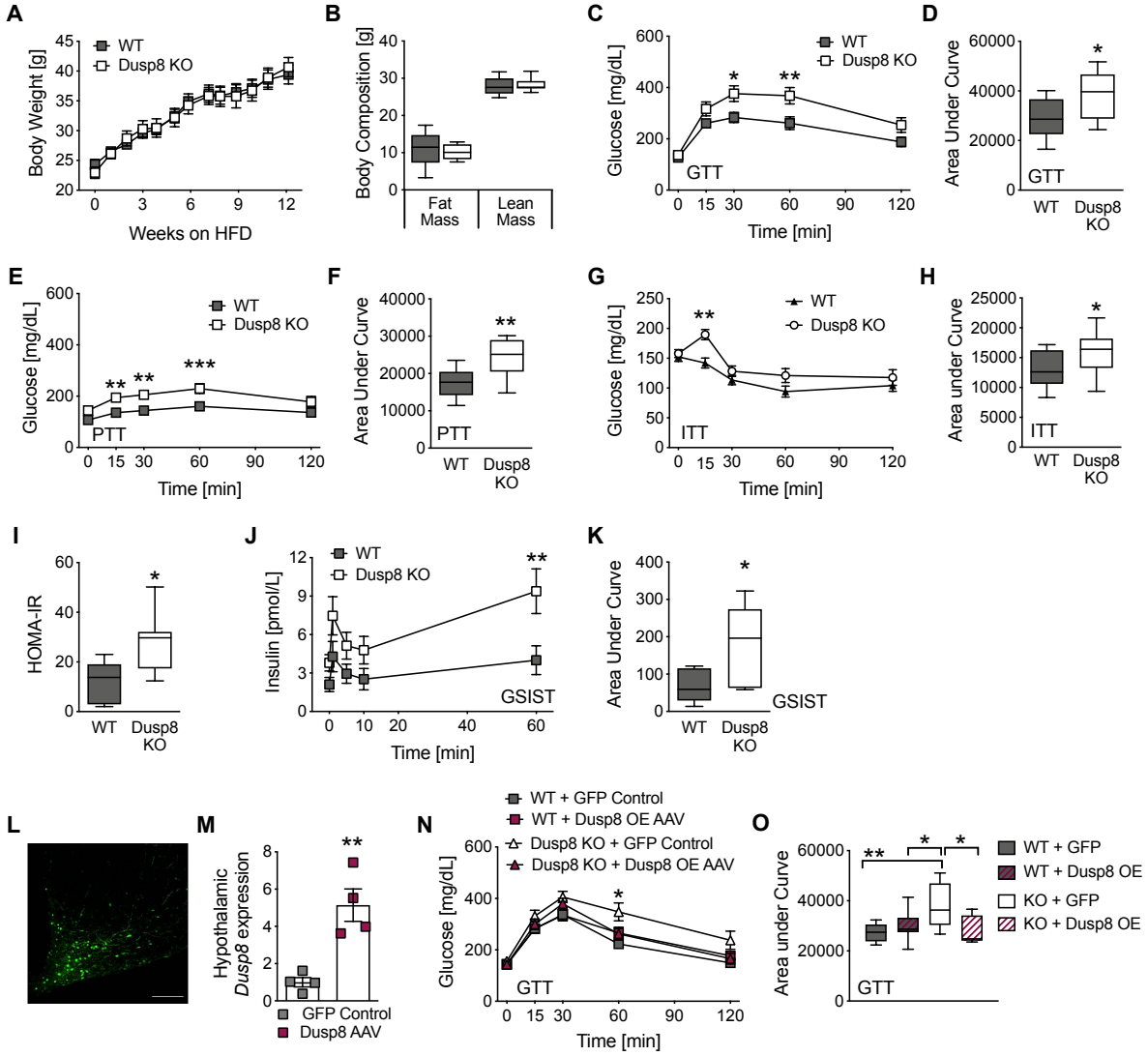

Figure 2: HFD-induced glucose intolerance in global male Dusp8 KO mice is reversed by hypothalamic Dusp8 overexpression.

Male Dusp8 WT (n=14) and KO (n=9) littermates were subjected to 45% HFD feeding and evaluated for **A)** body weight gain over 12 wks and for **B)** fat mass and lean mass after 13 wks of HFD exposure. **C-H)** Glucose tolerance (GTT), pyruvate tolerance (PTT) and insulin tolerance (ITT) tests were carried out after 12 wks, 14 wks or 13 wks of diet exposure, respectively (n=14 WT, n=9 Dusp8 KO). **I)** After 16 wks of HFD exposure, fasting glucose and insulin levels were measured in male Dusp8 WT (n=5) and KO mice (n=7) to calculate the HOMA-IR as insulin (mg/dl) x glucose (mg/dl) / 405. **J,K)** Insulin secretion during an ivGTT was measured in an additional cohort of male Dusp8 WT and KO mice (n=6 each,17 wks HFD). **L)** Representative picture of GFP-AAV control virus injected into the MBH. **M)** Hypothalamic Dusp8 mRNA expression one week after AAV-mediated overexpression of Dusp8 or control GFP in the MBH of lean WT mice (n=4). **N,O)** Glucose tolerance tests were carried out 4 wks after AAV injections into the MBH of male Dusp8 WT and KO mice (n=10 WT + GFP-AAV, n=10 WT + Dusp8 OE AAV, n=8 Dusp8 KO + GFP-AAV, n=10 Dusp8 KO + Dusp8 OE AAV).

Data are shown as means ± s.e.m (A,C,E,G,J,N), as box-and-whisker-plots (B,D,F,H,I,K,O) or as scatter dot plot (M). Scale bar = 200 µm. *p<0.05, **p<0.01 and ***p<0.001; Two-Way ANOVA (A,C,E,G,J,N), Student's t-test (B,D,F,H,I,K,M) or One-Way ANOVA (O).

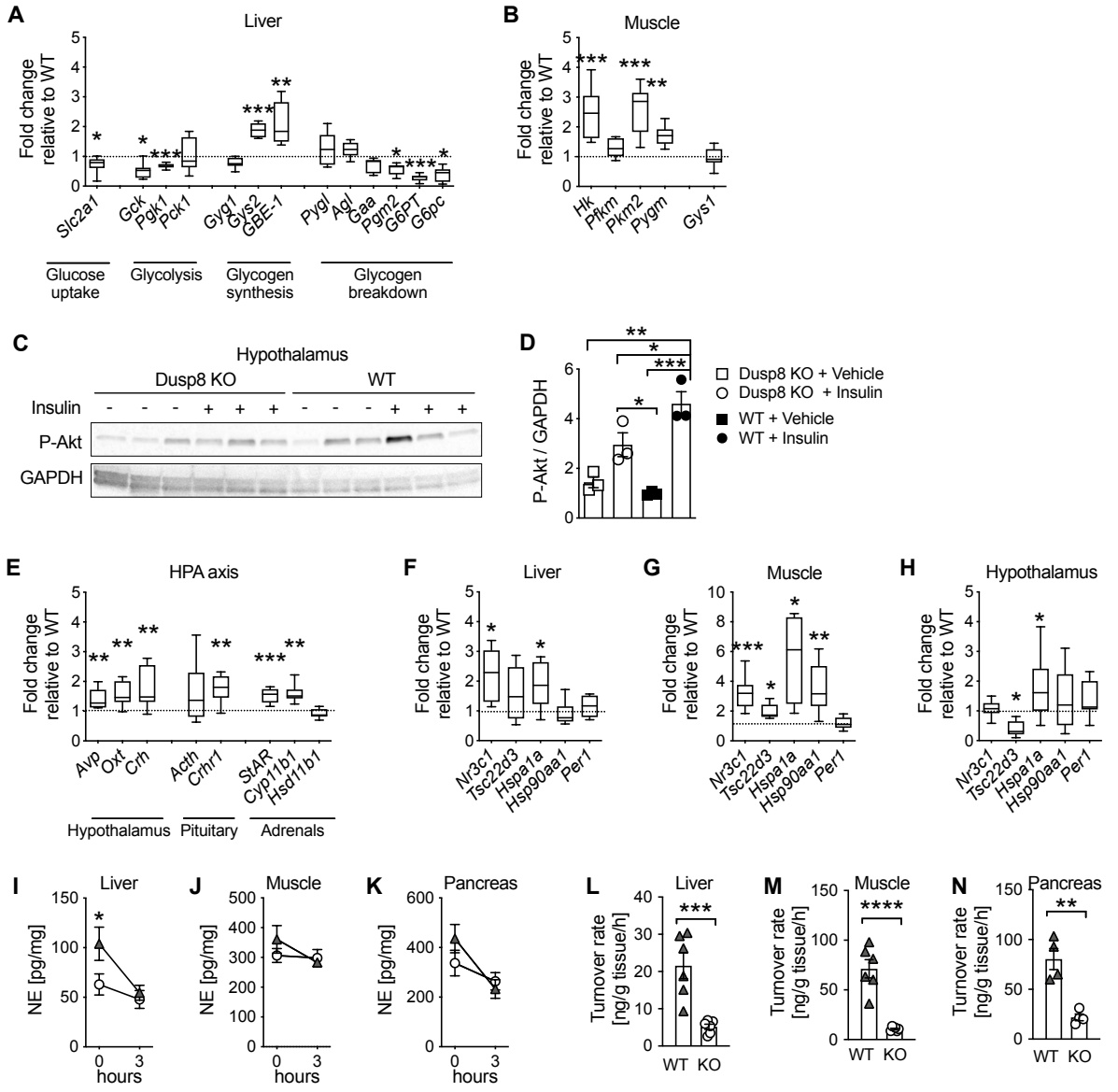

Figure 3: Elevated glucocorticoid action and impaired hypothalamic insulin sensitivity and sympathetic responsiveness in HFD-fed Dusp8 KO males.

A) Hepatic enzymes involved in glucose metabolism (n=7 WT, n=8 Dusp8 KO) and **B)** glucoregulatory enzymes in skeletal muscle (n=8 WT, n=8 Dusp8 KO) in 17-wks-HFD-fed, male Dusp8 KO mice relative to WT controls. **C)** Representative Western Blot and **D)** densitometric analysis of phosphorylated Akt relative to GAPDH in hypothalami of HFD-fed (17 wks) Dusp8 KO and WT males that were acutely injected with 3 IU insulin/kg BW or saline as control and sacrificed 8 min later (n=3). **E)** Gene transcripts related to HPA axis regulation measured in the hypothalamus (n=8 WT, n=8 Dusp8 KO) and pituitary (n=8 WT, n=8 Dusp8 KO) as well as enzymes involved in steroid synthesis measured in the adrenals (n=8 WT, n=7 Dusp8 KO) of 17-wks-HFD-fed mice. Tissue-specific glucocorticoid action in **F)** liver, **G)** muscle and **H)** hypothalamus (n=8 WT, n=8 Dusp8 KO) analyzed by qPCR. **I-K)** Norepinephrine (NE) tissue content before and 3 hrs after a-MPT injection and **L-N**) NE turnover rates in the liver, soleus and pancreas of male Dusp8 WT and KO mice exposed to HFD for 16 wks (n=6 for liver and soleus, n=4 for pancreas).

Data are shown as box-and-whisker-plots (A,B,E-H), as scatter dot plots (D,L-N) or as means ± s.e.m. (I-K). *p<0.05, **p<0.01, ***p<0.001 and ****p<0.0001; Student's t-tests (AB,E-H,L-N), One-Way ANOVA (D) or Two-Way ANOVA (I-K).

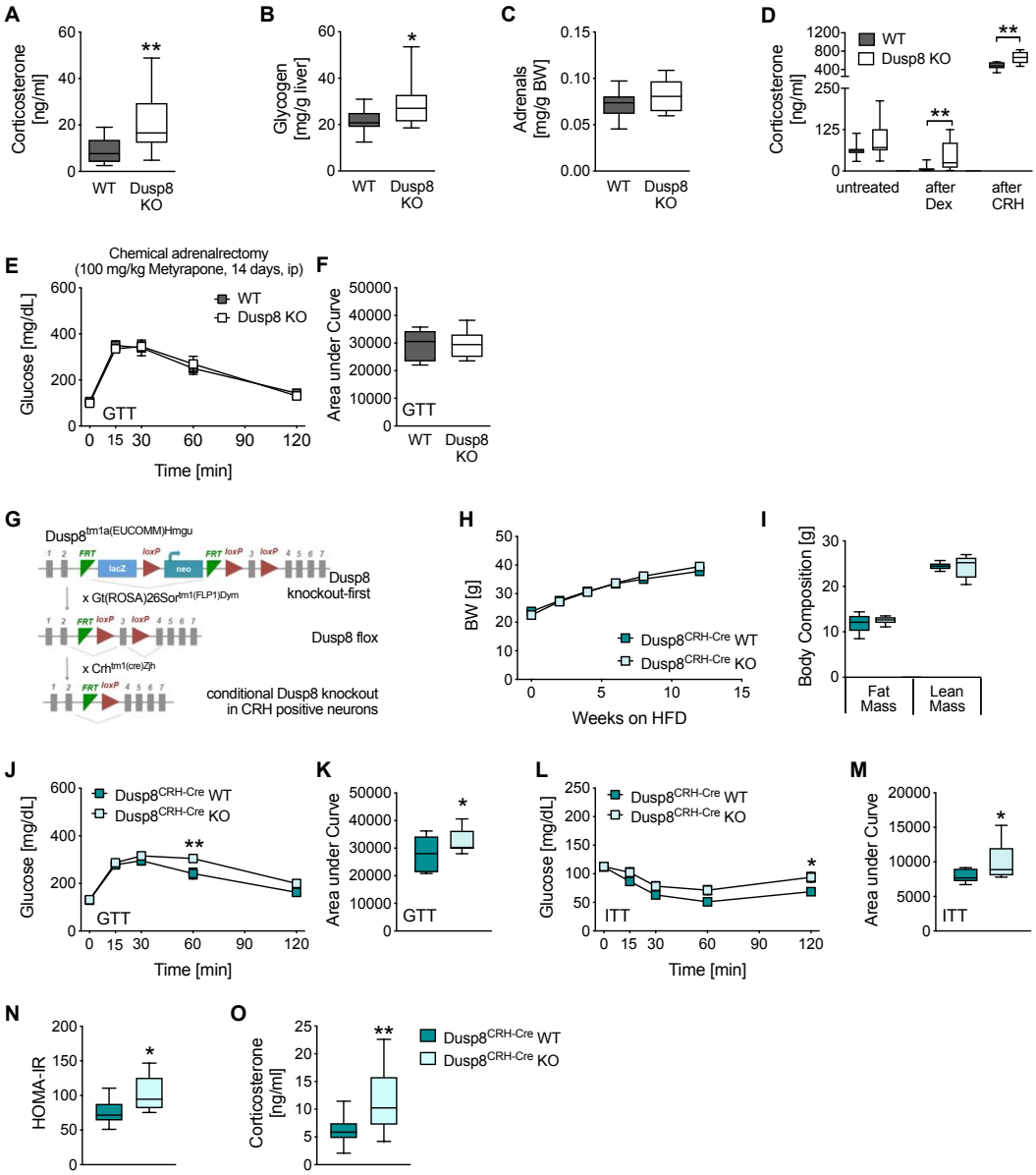

Figure 4: Chronic hypercorticosteronemia drives impaired glucose intolerance in HFD-fed male Dusp8 KO mice in a CRH neuron specific manner.

A) Plasma corticosterone levels in male mice sacrificed under basal conditions at 9 am (n=11 WT, n=12 Dusp8 KO; 17 wks HFD). **B)** Liver glycogen levels and **C)** adrenal weight normalized to body weight were determined after exposure to HFD for 17 wks (n=15 WT, n=14 Dusp8 KO). **D)** Plasma corticosterone levels of HFD-fed Dusp8 KO (n=11) and WT (n=11) males that were subjected to a combined Dex/CRH test with pharmacological suppression of adrenocortical activity by dexamethasone (0.05 mg/kg BW) and a subsequent stimulation with CRH (0.15 mg/kg BW). **E,F)** Glucose tolerance test (GTT) was carried out after 14 days of daily metyrapone injections (ip, 100 mg/kg BW) in male, HFD-fed Dusp8 WT (n=5) and KO (n=6) mice. **G)** Schematic for the generation of conditional, CRH neuron-specific Dusp8 KO mice **H)** Body weight gain over a total of 12 wks, and **I)** fat mass and lean mass of male Dusp8$^{CRH\text{-}Cre}$ WT (n=11) and KO (n=11) littermates after 12 wks HFD feeding. **J-M)** Glucose tolerance (GTT) and insulin tolerance tests (ITT) were carried out after 12 wks or 13 wks of HFD exposure, respectively (n=7 WT, n=9 Dusp8$^{CRH\text{-}Cre}$ KO). **N)** HOMA-IR of male Dusp8$^{CRH\text{-}Cre}$ WT (n=11) and KO mice (n=11) after 14 wks HFD exposure. **O)** Plasma corticosterone levels of male Dusp8$^{CRH\text{-}Cre}$ WT (n=14) and KO mice (n=20) after 14 weeks HFD exposure.

Data are shown as box-and-whisker-plots (A-D,F,I,K,M-O) or as means ± s.e.m. (E,H,J,L). *p<0.05, and **p<0.01; Student's t-test (A-D,F,I,K,M-O) or Two-Way ANOVA (E,H,J,L).

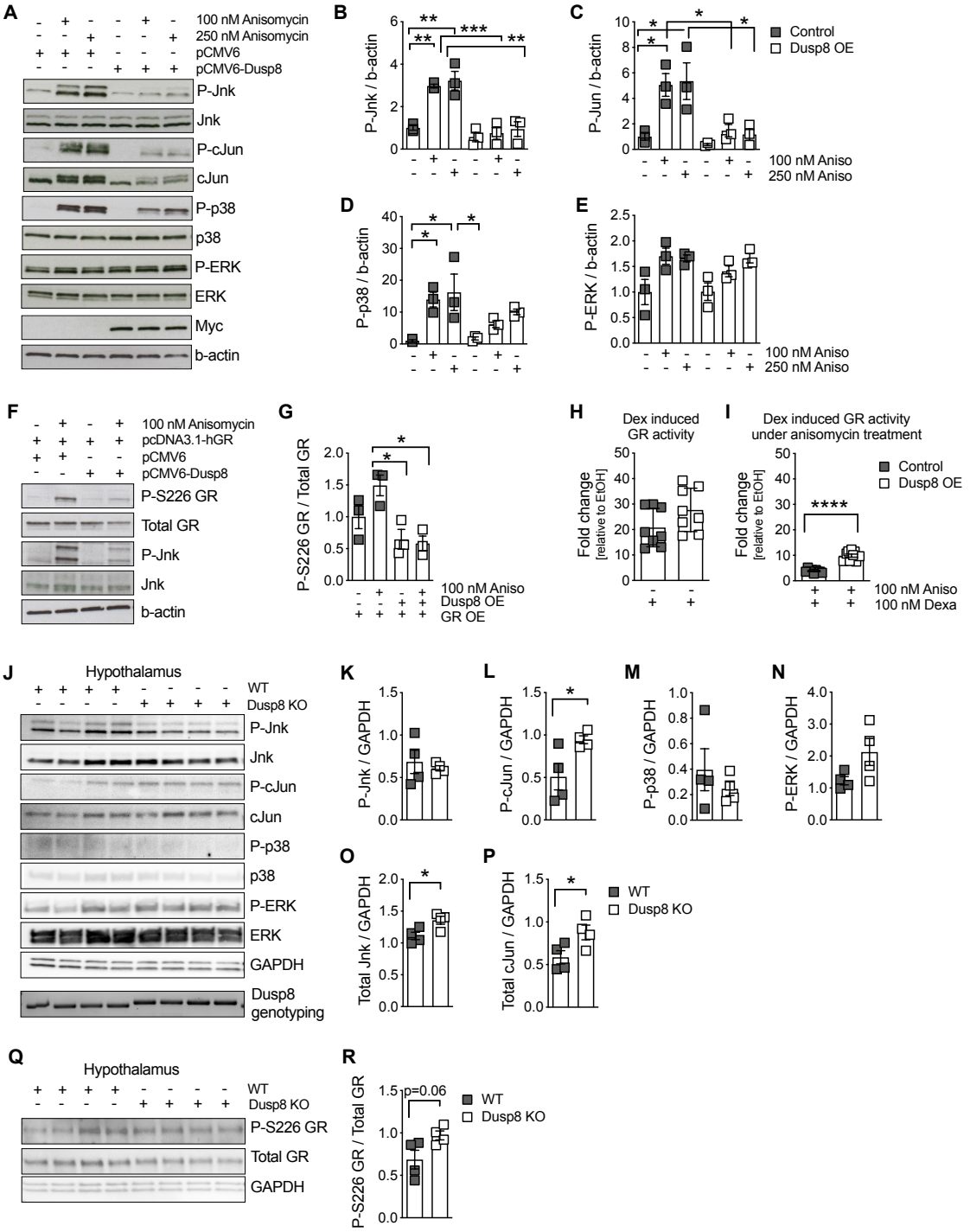

Figure 5: The Jnk-specific phosphatase Dusp8 is ameliorating the inhibitory effect of Jnk signaling on glucocorticoid action.

A) Representative Western Blot of an acute stimulation with MAPK activator anisomycin (30 min) in Hek293 cells with Dusp8 overexpression (OE, confirmed by presence of Myc), compared to pCMV6 control vector. Densitometric analysis of anisomycin-induced phosphorylation of **B)** Jnk, **C)** cJun **D)** p38 and **E)** ERK relative to beta-actin (n=3). **F)** Representative Western Blot and **G)** densitometric analysis of Hek293 cells with hGR OE and/or Dusp8 OE that were stimulated ± anisomycin (30 min) and then analyzed for phosphorylated GR at Ser226 relative to total GR (n=3). **H)** GR luciferase reporter assay activity in Hek293 cells overexpressing Dusp8 or an empty control plasmid stimulated with dexamethasone (5h, n=3 in biological triplicates). **I)** Dexamethasone-induced GR luciferase reporter assay activity in Hek293 cells with Dusp8 OE that were pre-treated with anisomycin (O/N, n=3 in biological triplicates).

J) Western Blot of hypothalami of HFD-fed (16 wks) male Dusp8 KO and WT mice (n=4 each). Genotypes were confirmed by PCR followed by agarose gel electrophoresis (WT=370 bp, KO=430 bp). **K-P)** Densitometric analysis of phosphorylated Jnk, cJun, p38 and ERK as well as total protein levels of Jnk and cJun relative to GAPDH (n=4 WT, n=4 KO; 16 wks HFD). **Q)** Western Blot and **R)** densitometric analysis of phosphorylated GR at Ser226 relative to total GR in hypothalami of male Dusp8 KO (n=4) and WT mice (n=4).
Data are shown as scatter dot plots. *p<0.05, **p<0.01, ***p<0.001 and ****p<0.0001; One-Way ANOVA (B-E,G) or Student's t-test (H,I,K-P,R).

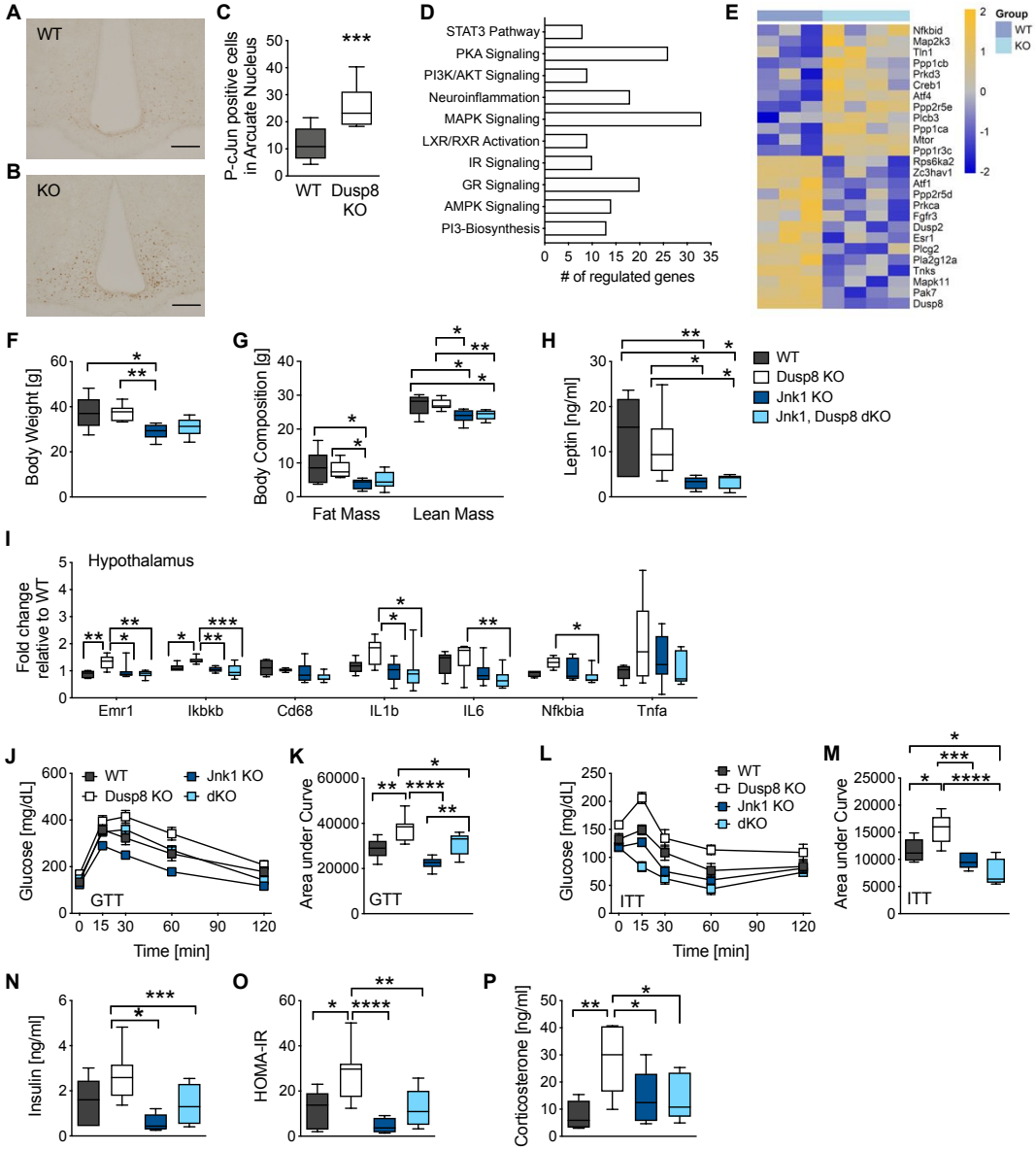

Figure 6: Glucose intolerance in HFD-fed male Dusp8 KO mice is mediated by Jnk.

Representative immunohistochemical detection of cJun phosphorylation in hypothalamic slices of male **A)** WT (n=14) and **B)** Dusp8 KO (n=9) littermates after 18 wks of HFD feeding and **C)** counting of positive stained nuclei. **D)** Pathway enrichment and **E)** heat map for MAPK signaling genes including Dusp8 from microarray analyses of laser-capture microdissected ARC of HFD-fed Dusp8 KO (n=4) and WT (n=3) mice. Relative gene expression values are shown across samples (z-scales to mean expression per row). **F)** Body weight and **G)** body composition, **H)** plasma leptin levels and **I)** markers of hypothalamic inflammation of male Dusp8 KO (n=7), Jnk1-Dusp8 dKO (n=9) and Jnk1 KO (n=8) mice relative to WT controls (n=6) were measured after 18 wks of HFD exposure.

J-M) Glucose tolerance (GTT) and insulin tolerance tests (ITT) were carried out after 16 wks or 17 wks of HFD exposure, respectively (n=6 WT, n=7 Dusp8 KO, n=8 Jnk1 KO, n=9 dKO). **N)** Plasma insulin levels were measured in WT (n=6), Dusp8 KO (n=7), Jnk1-Dusp8 dKO (n=9) and Jnk1 KO mice (n=8) after 18 wks of HFD exposure to calculate the HOMA-IR (**O**). **P)** Plasma corticosterone levels were measured in WT (n=6), Dusp8 KO (n=7), Jnk1-Dusp8 dKO (n=9) and Jnk1 KO mice (n=7) after 18 wks of HFD.

Data are shown as box-and-whisker-plots (C,F-I,K,M-P) or as means ± s.e.m. (J,L). Scale bar = 200 µM. *p<0.05, **p<0.01, ***p<0.001 and ****p<0.0001; Student's t-test (C), One-Way ANOVA (F-I,K,M-P) or Two-Way ANOVA (J,L).

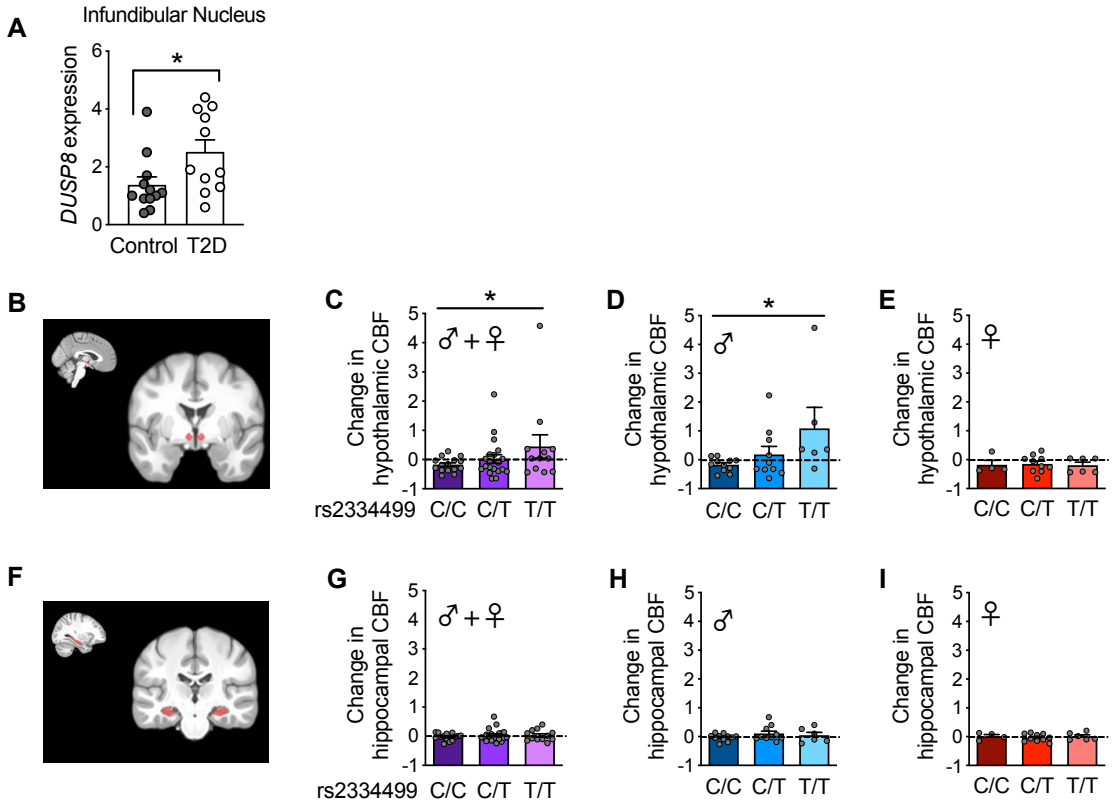

Figure 7: Increased Dusp8 expression in the infundibular nucleus of T2DM patients and hypothalamic insulin resistance in humans carrying the Dusp8 diabetes-risk allele.

A) *DUSP8* expression in the infundibular nucleus of humans without (n=12 control) or with T2D (n=11). **B**) Representative MRI brain images indicate the location of the hypothalamic region on the anatomical template in red. Intranasal insulin in healthy normal-weight individuals is known to decrease cerebral blood flow in the hypothalamus (30). Here, we extracted the relative change in cerebral blood flow (after insulin spray divided by before spray) to investigate insulin action in the hypothalamus based on the *DUSP8* SNP rs2334499 genotypes. **C)** The hypothalamic insulin response is displayed as the change in regional cerebral blood flow (CBF) after 160 U nasal insulin. Colours represent the *DUSP8* rs2334499 genotypes (n=15 major allele (C/C), n=20 heterozygous (C/T), n=12 minor allele (T/T)) in all subjects. CBF levels after stratification for sex are displayed for **D)** male (n=11 C/C, n=10 C/T, n=6 T/T) and **E)** female (n=4 C/C, n=10 C/T, n=6 T/T) *DUSP8* SNP rs2334499 carriers. F) Represetative MRI brain images with the hippocampal region displayed in red. The change in hippocampal CBF to intranasal insulin is displayed for **G)** all subjects, **H)** only men and **I)** only female participants.

Data are shown as scatter dot plots. *p<0.05; Wilcoxon rank-sum test (A) or multiple linear regression analysis (C-E,G-I).